Investigation into a role for the primitive streak in development of the murine allantois

Karen M. Downs*, Elissa R. Hellman, Jacalyn McHugh, Kathryn Barrickman and Kimberly E. Inman

Department of Anatomy, University of Wisconsin-Madison Medical School, 1300 University Avenue, Madison, WI 53706, USA
*Author for correspondence (e-mail: kdowns@facstaff.wisc.edu)

Accepted 25 September 2003

Development 131, 37-55
Published by The Company of Biologists 2004
doi:10.1242/dev.00906

Summary

Despite its importance as the source of one of three major vascular systems in the mammalian conceptus, little is known about the murine allantois, which will become the umbilical cord of the chorio-allantoic placenta. During gastrulation, the allantois grows into the exocoelomic cavity as a mesodermal extension of the posterior primitive streak. On the basis of morphology, gene expression and/or function, three cell types have been identified in the allantois: an outer layer of mesothelial cells, whose distal portion will become transformed into chorio-adhesive cells, and endothelial cells within the core.

Formation of endothelium and chorio-adhesive cells begins in the distal region of the allantois, farthest from the streak. Over time, endothelium spreads to the proximal allantoic region, whilst the distal outer layer of presumptive mesothelium gradually acquires vascular cell adhesion molecule (VCAM1) and mediates chorio-allantoic union. Intriguingly, the VCAM1 domain does not extend into the proximal allantoic region. How these three allantoic cell types are established is not known, although contact with the chorion has been discounted.

In this study, we have investigated how the allantois differentiates, with the goal of discriminating between extrinsic mechanisms involving the primitive streak and an intrinsic role for the allantois itself. Exploiting previous observations that the streak contributes mesoderm to the allantois throughout the latter's early development, microsurgery was used to remove allantoises at ten developmental stages. Subsequent whole embryo culture of operated conceptuses resulted in the formation of regenerated allantoises at all time points. Aside from being generally shorter than normal, none of the regenerates exhibited abnormal differentiation or inappropriate cell relationships. Rather, all of them resembled intact allantoises by morphological, molecular and functional criteria. Moreover, fate mapping adjacent yolk sac and amniotic mesoderm revealed that these tissues and their associated bone morphogenetic protein 4 (BMP4) did not contribute to restoration of allantoic outgrowth and differentiation during allantoic regeneration.

Thus, on the basis of these observations, we conclude that specification of allantoic endothelium, mesothelium and chorio-adhesive cells does not occur by a streak-related mechanism during the time that proximal epiblast travels through it and is transformed into allantoic mesoderm. Rather, all three cell-types are established by mechanisms intrinsic to the allantois, and possibly include roles for cell age and cell position. However, although chorio-adhesive cells were not specified within the streak, we discovered that the streak nonetheless plays a role in establishing VCAM1's expression domain, which typically began and was thereafter maintained at a defined distance from the primitive streak. When allantoises were removed from contact with the streak, normally VCAM1-negative proximal allantoic regions acquired VCAM1. These results suggested that the streak suppresses formation of chorio-adhesive cells in allantoic mesoderm closest to it.

Together with previous results, findings presented here suggest a model of differentiation of allantoic mesoderm that invokes intrinsic and extrinsic mechanisms, all of which appear to be activated once the allantoic bud has formed.

Key words: Allantois, BMP4, Chorio-allantoic union, Cytokeratins, Differentiation, Endothelium, Gastrulation, Mesoderm, Mesothelium, Mouse, Placenta, Primitive streak, Regeneration, Umbilical cord, Vasculogenesis, VCAM1

Introduction

A major goal in developmental studies is to discover how embryonic cells differentiate into a vast array of cell types. In the mouse, it is thought that many critical decisions take place just before and during gastrulation, when the primary germ layers are established (Beddington, 1983).

Pre-eminent in germ layer formation is the primitive streak, a localized thickening in the midline of the epiblast (Bonnevie, 1950; Batten and Haar, 1979). Appearance of the streak defines the posterior end of the future fetus and thus, its anteroposterior axis. The streak is also thought to be where epiblast is transformed into endoderm and mesoderm, both of which are then directed to appropriate sites in the conceptus (Jolly and Ferester-Tadié, 1936; Snell and Stevens, 1966; Poelmann, 1981; Tam and Beddington, 1987; Lawson et al., 1991; Kinder et al., 1999).

Results of both tissue (Beddington, 1982; Copp et al., 1986; Tam and Beddington, 1987) and clonal (Lawson et al., 1991; Lawson and Pedersen, 1992) fate mapping experiments demonstrated that proximal epiblast, located at the embryonic/extraembryonic junction, ingresses into the nascent posterior streak, where it de-epithelializes to emerge as mesoderm (Batten and Haar, 1979; Bellairs, 1986). A large fraction of this mesoderm will be displaced into the extraembryonic region, and lines the exocoelomic cavity (Bonnevie, 1950; Lawson et al., 1991; Lawson and Pedersen, 1992). Shortly thereafter, additional extraembryonic mesoderm accumulates at the posterior angle between the amnion and yolk sac and becomes the allantoic bud (Bonnevie, 1950; Snell and Stevens, 1966) (reviewed by Downs, 1998). Thus, the posterior primitive streak is the allantois' immediate site of origin.

The allantoic bud enlarges into the exocoelomic cavity by a combination of proliferation (Ellington, 1985; Downs and Bertler, 2000), continuous deposition of mesoderm from the streak (Tam and Beddington, 1987; Downs and Bertler, 2000), and distal cavitation (Ellington, 1985; Brown and Papaioannou, 1993; Downs, 2002). During enlargement, two morphologically distinct cell populations are established within the allantois (Ellington, 1985; Downs et al., 1998): an outer layer of 'mesothelium', and an inner core of vascularizing mesoderm, defined initially by a plexus of endothelial cells. Formation of the endothelium occurs de novo within the allantois, beginning in its distal region with the appearance of FLK1 (KDR – Mouse Genome Informatics)-containing angioblasts (Downs et al., 1998). Specification of angioblasts and their morphogenesis into endothelial tubules then proceeds proximally to the base of the allantois, where nascent allantoic blood vessels amalgamate with those of the yolk sac and the fetus to create a vascular continuum throughout the conceptus (Downs et al., 1998). Ultimately, the allantoic vascular plexus will be remodeled into an umbilical artery and vein (Kaufman, 1992).

Although the timing of appearance of the mesothelium is not known, it has been proposed, on the basis of limited light microscopic data, that distalmost allantoic cells begin to flatten at approximately the neural plate stage (Downs et al., 1998). By 4-somite pairs, the allantoic projection is enveloped in a morphologically distinct mesothelium (Downs et al., 1998), the distal portion of which contains vascular cell adhesion molecule (VCAM1) (Gurtner et al., 1995; Kwee et al., 1995; Downs et al., 2001; Downs, 2002), required for chorio-allantoic union (Gurtner et al., 1995; Kwee et al., 1995). Aside from VCAM1, the only other gene whose protein product has been clearly demonstrated in outer allantoic cells at all stages examined is *Ahnak* (Kingsley et al., 2001; Downs et al., 2002), although its significance there is not yet known.

On the basis of its ultimate morphology and function, the allantois must eventually contain at least two other cell types: vascular smooth muscle (Takahashi et al., 1996), common to all major arteries and veins, and mesenchymal cells that will provide a connective tissue matrix for the umbilical blood vessels. However, neither of these cell types has been identified in the developing allantois, nor is it known whether they differentiate from allantoic mesoderm or are contributed to the allantois by the chorion after these two tissues unite.

Intriguingly, unlike yolk sac mesoderm, whose transformation into blood islands is dependent upon contact with adjacent endoderm (Wilt, 1965; Miura and Wilt, 1970; Belaoussoff et al., 1998), allantoic mesoderm grows into the exocoelomic cavity as a physically isolated projection. It complexes with the chorion only after allantoic endothelium, mesothelium and chorio-adhesive cells have appeared (Downs and Gardner, 1995; Downs et al., 1998; Downs, 2002).

Thus, given the allantois' relative independence in the exocoelom, it was not clear how the allantois might differentiate. We envisioned at least two strategies. First, the allantois itself might contain intrinsic cues that direct its own differentiation. Second, as the posterior primitive streak is both the site of production of allantoic mesoderm and also initially continuous with it, we postulated that the streak might be integral to allantoic differentiation, specifying allantoic mesoderm as it formed therein, and/or once the allantoic bud had appeared.

Results of several studies support roles in differentiation for both of these tissues. When distal allantoic halves were placed into the exocoelomic cavity of synchronous hosts, donor allantoises united with the hosts' chorion at the appropriate time, despite lack of continuity with the proximal allantoic region and the posterior primitive streak (Downs and Gardner, 1995). Moreover, when allantoises were explanted and cultured in isolation, they invariably vascularized (Downs and Harmann, 1997; Downs et al., 1998) in a stereotypic distal-to-proximal sequence (Downs et al., 2001). Together, these observations suggested a mechanism of differentiation intrinsic to the allantois.

That the streak participates in differentiation of allantoic mesoderm was anticipated in at least two ways, each supported by experimental analysis. In the first, results of heterotopic transplantations suggested that the streak might specify proximal epiblast into particular allantoic cell types while it was being transformed into extraembryonic mesoderm. When nascent posterior mesoderm, the immediate precursor of extraembryonic mesoderm, including the allantois (Tam and Beddington, 1987; Lawson et al., 1991; Kinder et al., 1999), was removed from the primitive streak and transplanted to the distal region of hosts, it exhibited limited developmental potential, failing to colonize the somites of the ectopic site (Dunwoodie and Beddington, 2002). Moreover, when proximal allantoic mesoderm, having just emerged from the streak, was transplanted into a similar ectopic region (Downs and Harmann, 1997), it contributed only to blood vessels, and not to somitic mesoderm. Together, these results suggested that allantoic endothelial cells might be specified within the streak.

Results of a second set of observations suggested that the streak might influence allantoic differentiation after the bud had formed, for example, through factors emanating from a localized signaling center. Allantoic cells closest to the streak might remain initially undifferentiated, whereas those cells farther away would escape the streak's influence and differentiate [proposed by Downs and Harmann (Downs and Harmann, 1997)]. This possibility is consistent with the observation that differentiation of the allantois into endothelium and chorio-adhesive cells begins in the allantois' distal region (Downs and Harmann, 1997); although endothelium is eventually observed throughout the allantois (Downs et al., 1998), VCAM1's domain is restricted to the distal region at all time points examined (Gurtner et al., 1995;

Kwee et al., 1995; Downs et al., 2001; Downs, 2002). Thus, distance from the primitive streak might dictate where chorio-adhesive cells arise and are maintained.

Results of several studies have suggested that the posterior streak is indeed a site within which decisions are made that specify cell differentiation and fate, distinguishing extraembryonic from embryonic mesoderm and the future germ line. Intriguingly, the protein products of some homeobox genes, i.e. those transcription factors critical in the regulation of cell proliferation, differentiation, migration, organogenesis and pattern formation during embryogenesis (reviewed by Deschamps and Meijlink, 1992), appear to be involved, as described below.

First, that extraembryonic and embryonic mesoderm may be distinguished in the streak was suggested by expression studies of the homeobox gene, *Evx1*, and by analysis of genetic knockouts of the Polycomb-group homeobox gene, embryonic ectoderm development, or *Eed*. Throughout gastrulation, localization of Evx1 was limited to cells near and within the streak (Dush and Martin, 1992). Together with results of fate-mapping, which demonstrated that different types of mesoderm emerge from different axial levels of the streak (Tam and Beddington, 1987; Lawson et al., 1991; Lawson and Pedersen, 1992; Kinder et al., 1999), it was suggested that *Evx1* might play a role in establishing the downstream regulatory cascade required for specification of mesodermal cell fate. In a separate study, absence of the *Eed* gene product led to overproduction of extraembryonic mesoderm, whereas embryonic axial and paraxial mesoderm were missing in the mutants (Schumacher et al., 1996). Together, these observations support the notion that the posterior streak is a region where mesodermal type is specified.

Second, in addition to distinguishing extraembryonic from embryonic mesoderm, the posterior primitive streak is also the site where primordial germ cells (PGCs) are allocated (Chiquoine, 1954; Ozdzenski, 1967; Copp et al., 1986; Ginsburg et al., 1990; Lawson and Hage, 1994; Lawson et al., 1999; Saitou et al., 2002). A recent model has proposed that localized cell signaling within the posterior streak distinguishes extraembryonic mesoderm from nascent germ cells (Saitou et al., 2002). The distinction is thought to be achieved through suppression of *Hox* gene expression in some cells, thereby allowing them to escape a somatic, or extraembryonic mesodermal, cell fate and retain pluripotency, becoming PGCs. However, the precise nature of these signals is not known.

Thus, to discriminate between roles for the allantois and the primitive streak in differentiation of allantoic mesoderm, we exploited several observations. First, microsurgical removal of allantoises during their pre-fusion phase had previously demonstrated that the streak continuously contributes mesoderm to the allantois, as reflected in the formation of allantoic regenerates over a 20-hour time period (Downs and Bertler, 2000). We reasoned that, if allantoic cell types were specified within the streak, one or more of them might be missing in the regenerates. Alternatively, if the regenerates appeared relatively normal, then we might conclude that differentiation occurred by cues intrinsic to the allantois. A combination of experimental approaches could be used to test this: morphology and the presence of FLK1 within the regenerates' core would identify endothelial cells; morphology and localization of cytokeratins to the outer surface of the regenerates might identify mesothelium; and the functional chorio-allantoic union assay (Downs and Gardner, 1995) together with VCAM1 in outer distal cells of the regenerates would indicate the presence of chorio-adhesive cells (Downs et al., 1998; Downs, 2002). Second, regional specificity of VCAM1 might be established by the streak once the allantoic bud had formed. To test this, whole allantoises could be microsurgically removed and their polarity reversed within the exocoelom. Loss of contact with the streak might induce proximal mis-expression of *Vcam1*, thereby identifying a role for the streak in localizing chorio-adhesive cells to the distal allantoic region.

Results of this study provide evidence that specification of endothelium, mesothelium and chorio-adhesive cells does not occur within the streak. Nevertheless, they do support a role for the streak in establishment, and possibly maintenance, of the *Vcam1* expression domain once the bud has formed. Further, ontogeny of mesothelium does not begin in the distal region, as previously posited (Downs et al., 1998); rather, a variety of junctional complexes are visible throughout the allantoic periphery as soon as the bud appears in the exocoelom.

On the basis of these and previous results, a model of allantoic development is proposed that involves information intrinsic to the allantois, as well as signaling from the primitive streak once the allantoic bud has formed.

Materials and methods

Mouse strains, dissection, staging, whole embryo culture

Light-reversed conditions (dark period: 13.00-1.00) maintained all mice used in this study. Matings between F1 hybrids (C57Bl/6×CBA) (Jackson Laboratory) produced an F2 generation that was used as standard 'wild-type' material in most experiments. For transplantation experiments, *lacZ/+* labeled tissue was obtained by mating F1 hybrid females with ROSA26 males of F1 genetic background and homozygous for two copies of the ubiquitously expressed *lacZ* transgene (Friedrich and Soriano, 1991). Dissection, staging, whole embryo culture and morphological scoring were previously described (Downs and Davies, 1993; Downs and Gardner, 1995; Downs and Harmann, 1997; Downs et al., 1998; Downs and Bertler, 2000; Downs et al., 2001; Downs, 2002). Most experiments involved conceptuses encompassing all pre-fusion stages, defined from the time of the appearance of the allantoic bud through six-somite pairs, when fusion with the chorion was completed (Downs and Gardner, 1995) (approximately 7.25-8.5 days postcoitum, dpc). In all experiments, operated conceptuses were cultured alongside stage-matched unoperated ones, the latter of which verified culture conditions appropriate for gene expression, endothelialization and chorio-allantoic union. Except for experiments involving AlexaFluor594-conjugated Concanavalin A, described below, no significant differences in embryo size or morphological differentiation were noted. After scoring, conceptuses were prepared for histology and immunostaining (Downs and Harmann, 1997; Downs et al., 1998; Downs et al., 2001; Downs, 2002; Downs et al., 2002), described below.

Microsurgical procedures

Creation of allantoic regenerates

Allantoic regenerates were created throughout pre-fusion stages by aspirating whole allantoises through a mouth-held microcapillary after puncturing the anterior yolk sac (Downs and Gardner, 1995; Downs and Bertler, 2000) and culturing operated conceptuses for variable time periods. The base of the allantois had previously been

defined as the point of insertion of the allantois into the yolk sac and amniotic mesoderms (Ozdzenski, 1967; Downs and Harmann, 1997). Complete removal of the allantois was verified by visual inspection before culture.

Reversed polarity of whole allantoises

For reversed polarity experiments, whole *lacZ/+* donor allantoises were introduced into wild-type host conceptuses whose own allantoises had been removed by aspiration. Where control donor allantoises were placed in normal orientation within the hosts' exocoelom (i.e. distal tips toward the chorion), their proximal ends were labeled by brief (10 seconds) immersion in DiI′/DiIC18(3) (1,1′-dioctadecyl-3,3,3′-tetramethyindocarbocyanine perchlorate, MW 933.88, Molecular Probes, Eugene, OR, USA: D-282) as previously described (Downs et al., 2001). Where donor allantoises were introduced into the hosts' exocoelom with reversed polarity (i.e. proximal ends toward the chorion), their tips, rather than their proximal ends, were labeled. Orientation of donor allantoises was monitored immediately before, during and at the end of the culture period either in the light microscope, as the dye was visible as a pink color on the surface of the cells, or in the inverted compound microscope with brief rhodamine excitation (G2-A filter cube, excitation 535/50, emission 590; Chroma, Rockingham, VT, USA); proximodistal orientation was scored with respect to the anteroposterior and left-right body coordinates. In some experiments, wild-type allantoic tissue confirmed results obtained with *lacZ/+* allantoises, as X-gal could obscure the immunostain in the latter.

Isolation and culture of allantoic subregions

Allantoic subregions were excised from whole allantoises at all pre-fusion stages with the aid of glass scalpels (Beddington, 1987) and either introduced into the exocoelom of host conceptuses whose own allantois had been removed, or cultured in isolation either directly onto tissue culture plastic or free-floating, as previously described (Downs and Harmann, 1997; Downs et al., 1998; Downs et al., 2001).

X-gal- and immunostaining

X-gal staining identified *lacZ/+* tissue after fixation in 4% paraformaldehyde, as previously described (Downs and Harmann, 1997; Downs et al., 1998; Downs et al., 2001; Downs, 2002), with the exception that exposure to X-gal was for 2 or 6 hours. Bouin's fluid was used to fix all conceptuses that did not involve X-gal staining. All fixed material was embedded in paraffin wax and sectioned at a thickness of 6 μm. All intact allantoic profiles presented in this study are sagittal views.

Antibodies against FLK1, VCAM1, BMP4 (Santa Cruz Biotechnology, Santa Cruz, CA, USA) and cytokeratins (DAKO Corporation, Carpinteria, CA, USA) were used in indirect immunohistochemistry. As the literature provided no guidance concerning expression of specific cytokeratins in the allantois, antibodies against a wide spectrum were used. Antibody binding was performed for variable times at room temperature or 4°C, and ready-to-use reagents detected the antibody-antigen complexes (streptavidin-horseradish peroxidase, Vector Laboratories, Burlingame, CA, USA; diaminobenzoate (DAB), DAKO). Pre-binding control peptides to anti-FLK1 and anti-VCAM1 served as negative controls and were previously described (Downs et al., 1998; Downs et al., 2001; Downs, 2002); increasing concentrations of control peptide to anti-BMP4 (Santa Cruz Biotechnology), which was raised against the N-terminal region of the protein, confirmed antibody specificity. Histological sections were also incubated in the absence of antibody in all immunolocalization experiments, including those for cytokeratins for which no control peptide was commercially available. However, antibodies against cytokeratins strongly reacted against trophoblast giant cells, in agreement with previous findings (Hashido et al., 1991; Jaquemar et al., 2003), thereby providing an internal control for antibody specificity. X-gal-stained material was counterstained in nuclear fast red; most other material was stained either in hematoxylin/eosin (H/E) or hematoxylin alone.

Concanavalin A

Lectin-conjugated compounds have previously been used to fate-map cells which border a cavity (Tam and Beddington, 1987). After a brief microspin to remove particulate, AlexaFluor594-conjugated Concanavalin A (absorbance, 590 nm; emission, 617 nm; 2.5-5 mg/ml sterile PBS; Molecular Probes) was gently blown into the exocoelomic cavity of pre-fusion conceptuses via a mouth-held microcapillary in eight separate experiments. After 1 minute of exposure, labeled exocoeloms were repeatedly rinsed with the aid of a mouth-held microcapillary for 3-5 minutes, after which allantoises were removed. ConA labeling of both the mesoderm lining the exocoelomic cavity and the entire surface of isolated allantoises was confirmed (G2-A filter cube, described above, mercury lamp had logged 0-100 hours). After 8-12 or 20-24 hours of culture, allantoic regenerates and unoperated labeled and unlabeled control allantoises were examined by peeling away yolk sacs, cutting out allantoises with a glass scalpel, and viewing them, the yolk sacs and the amnions in both whole-mount and squashed preparations under fluorescence.

To confirm that labeled cells both proliferated and contributed label to their progeny, ConA-labeled headfold- and early somite-stage yolk sacs were isolated, rinsed and treated with a mixture of trypsin and pancreatin (Downs and Harmann, 1997) for 2 minutes on ice, after which the enzyme was inactivated in dissection medium. The mesodermal and endodermal cell layers were then separated via aspiration through a small diameter microcapillary (Beddington, 1987). The cell layers were placed separately into sterile Eppendorf tubes, and further enzyme-treated (15 minutes on ice) to obtain single cell suspensions, which were briefly spun down, resuspended in dissection medium, and plated onto 8-well chamber slides (Nunc Permanox; Nunc, Naperville, IL, USA) containing 0.4 ml culture medium. After 5 hours, floating cells were removed, the adherent cells were fed, counted and cultured for 20 hours more, at which time the medium was again replaced, and the adherent labeled cells counted. In addition, we verified that AlexaFluor ConA did not inhibit cell motility by plating labeled aspirated allantoises (two experiments, n=10) directly onto tissue culture plastic (Downs et al., 2001) and demonstrating the presence of labeled mesothelial outgrowth at 8 and subsequently 20 hours.

In eight experiments, all 21 unlabeled, unoperated conceptuses were normal at the end of the culture period and negative for ConA. Of 27 control conceptuses whose allantois had been labeled but not removed from the exocoelom, one fetus (3.7%) was abnormal in that the ConA-labeled allantois had fused with the yolk sac rather than with the chorion. Of the 72 conceptuses whose allantoises had been labeled, removed and subsequently regenerated, none were abnormal, although one conceptus (1.4%) was dead; a subset of these (n=22) was measured in the dissection microscope (see next section) and their average length compared with that of unlabeled regenerated allantoises (n=6). In a final set of control experiments, allantoises were removed prior to labeling exocoelomic cavities (two experiments, eight conceptuses, two fetuses of which were abnormal after culture) to ascertain the probable labeling pattern if yolk sac/amniotic mesodermal cells crawled over the primitive streak during regeneration, as well as to verify persistence of label in the regenerates.

Measurement of allantoises and the VCAM1-free region

The length of some 20- and 6-hour allantoic regenerates and unoperated allantoises was measured in the dissection microscope immediately after culture, by means of an eyepiece reticule, and plotted (Fig. 2A,B) or reported in Results. The average length and standard error of the mean (s.e.m.) of histologically prepared and sectioned allantoises and their VCAM1-negative regions were obtained from the longest three sagittally oriented sections after

photography, computer scanning (Adobe Photoshop) and printing (Fig. 4).

Transmission electron microscopy

Conceptuses were dissected and staged as described above. Embryos at the neural plate (early and late bud), headfold (early and late), and 4-somite pair stages were immersion fixed in Karnovsky's fixative (2% paraformaldehyde, 2.5% glutaraldehyde in 0.1 M $NaPO_4$ buffer, pH 7.4) for 2 hours at 4°C, after which they were washed in rinsing buffer (0.1 M $NaPO_4$) and postfixed in 2% osmium tetroxide (OsO_4) buffered in 0.1 M $NaPO_4$ for 1 hour at room temperature. Postfixed samples were washed in rinsing buffer and dehydrated in a graded series of ethanols for 7-12 minutes at room temperature, with a final dehydration in propylene oxide as a transition solvent. Dehydrated samples were infiltrated between 20-65°C in a 1:1 mixture of Embed-812 and Spurr's Low Viscosity embedding media (Electron Microscopy Sciences, Fort Washington, PA, USA) that included propylene oxide. Semi-thin (3 μm) serial sections of sagittally oriented allantoises were collected and dried on slides. Target sections were selected and remounted on polymerized resin Beem capsule stubs in preparation for thin sectioning. Ultrathin sections (70 nm) were collected on pioloform-coated 2×1 mm aperture copper electron microscope grids (Electron Microscopy Services, Fort Washington, PA, USA). Ultrathin sectioning (100-500 nm) was performed on a Reichert-Jung Ultracut E ultramicrotome. The sections were post-stained in uranyl acetate and lead citrate. The samples were viewed and documented on a Philips CM120 at 80 kV.

Statistical analyses

The Student's two-way *t*-test (Mini-Tab, equal variances assumed, Confidence Interval=95%) determined significant differences ($P<0.05$) between treatment categories wherever relevant in this study.

Results

The primitive streak is active during pre-fusion allantoic development

Results of earlier studies suggested that allantoises microsurgically removed from the conceptus prior to their union with the chorion would regenerate (Downs and Gardner, 1995). Later, allantoic regeneration was exploited to determine when and how much mesoderm was added to the allantois by the streak (Downs and Bertler, 2000). Findings revealed streak activity at all pre-fusion stages, although mesoderm contribution decreased with increasing developmental age. On the basis of these observations, we hypothesized that allantoic regenerates would be a powerful experimental means by which to investigate the effect of streak activity on differentiation of allantoic mesoderm. The rationale was that, if any of the regenerates lacked certain cell populations, then specification of the missing cell type(s) might have occurred within the streak at or slightly later than the time of allantoic removal.

To ensure that regenerates formed at all pre-fusion stages, whole allantoises were removed, exposing the subjacent posterior primitive streak (Fig. 1A-E). After 20 hours in culture, operated conceptuses were examined in the dissection microscope and regenerates were measured. Regeneration was found at all developmental stages, but only a few regenerates grew far enough to unite with the chorion (Fig. 2A). The average length of 'unfused' regenerates was remarkably similar between the neural plate and 5-somite pair stages (501.5±21.7 μm, $n=54$), but significantly shorter ($P<0.000$) than unoperated controls (924.7±17.6 μm, $n=44$). The average length of regenerates formed from the 6-somite pair stage was significantly shorter (244.6±66 μm, $n=6$) than the other regenerates ($P=0.002$, Student's two-way *t*-test with 5-somite pair regenerates). Thus, on the basis of these findings, we conclude that, during pre-chorionic fusion stages, the primitive streak is active at all time points, producing regenerated allantoises.

Twenty-hour allantoic regenerates exhibit normal differentiation and can unite with the chorion

To establish whether endothelium, mesothelium and chorio-adhesive cells were present in all of the 20-hour regenerates, histological and immunohistochemical analyses were performed. All regenerates were completely enveloped by mesothelium, and all contained evidence of a vascularizing core that extended down their length (Fig. 1F), in accord with the morphology of normal ex vivo counterparts at equivalent developmental ages (≥7-somite pairs) (Downs et al., 1998).

FLK1 was found in the endothelial cells of 20-hour regenerates, and never in the mesothelium (Fig. 1G) (Downs et al., 1998). Similarly, VCAM1 was appropriately localized to the distal two-thirds of all allantoic regenerates, which included the mesothelium and some core cells (Fig. 1H) (Downs et al., 2001; Downs, 2002). Double immunohistochemistry revealed normal cell-cell relationships in the regenerates: VCAM1-positive cells were associated with, but distinct from, the FLK1-positive core vasculature, and absent from the proximal allantoic third (Fig. 1I-L) (Downs, 2002).

Of the 77 allantoic regenerates of Fig. 2A, a small number (22%) had undergone union with the chorion. In these, microscopic inspection revealed that the early steps of placentation were occurring: the chorio-allantoic fusion surfaces appeared to be breaking down, and the FLK1-positive allantoic vasculature was penetrating chorionic ectoderm (data not shown), as previously described (Downs, 2002). Of the remaining regenerates, none grew far enough to unite with the chorion. To discover whether these were nonetheless functionally normal, *lacZ/+* unfused regenerates were aspirated at 20 hours, placed into the exocoelom of pre-fusion wild-type host conceptuses whose own allantoises had been microsurgically removed, and the operated hosts were cultured to just beyond 6-7-somite pairs, when all allantoises have normally united with the chorion (Downs and Gardner, 1995; Downs, 2002). In two experiments, 4/4 grafted X-gal-stained regenerated allantoises exhibited convincing union with the hosts' chorion (data not shown), suggesting functional adhesive capabilities.

Why some regenerates grew far enough to unite with the chorion could be explained by prolonged collapse of the exocoelomic cavity, possibly because the yolk sac puncture did not heal in a timely manner. As a consequence of reduced exocoelomic volume, they could have been brought into closer proximity to the chorion, thereby initiating union.

Thus, not only do regenerates demonstrate appropriate morphological and molecular properties, but they are also functionally competent, capable of uniting with the chorion if given the opportunity.

Formation of mesothelium

The normal morphological, molecular and functional profiles of 20-hour regenerates suggested that the primitive streak does

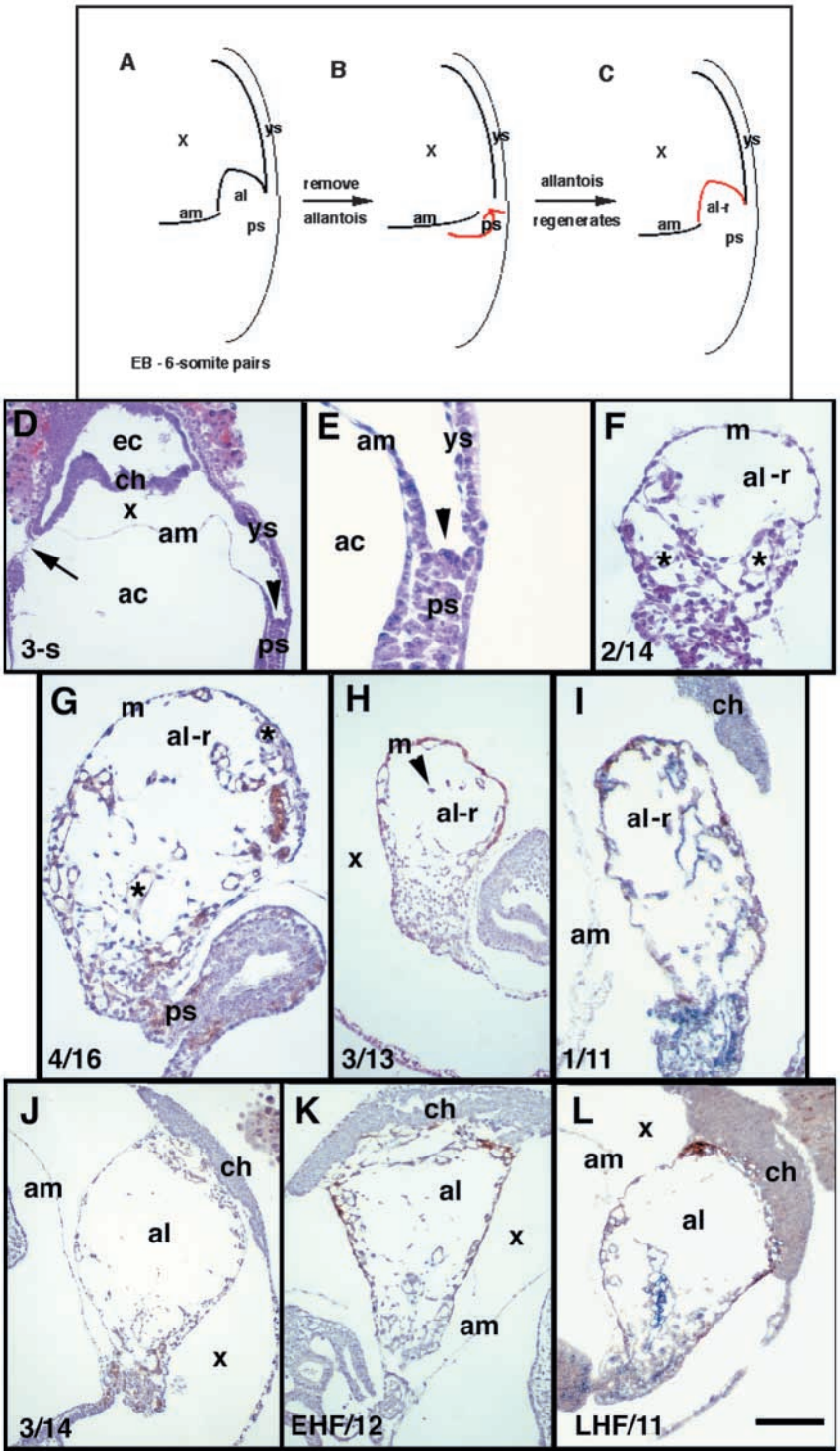

Fig. 1. Morphology and immunostaining in 20-hour allantoic regenerates. (A-C) Schematic drawings illustrate the formation of allantoic regenerates between the neural plate/early allantoic bud (EB) through 6-somite pair stages (lower left). (A-B) The allantois (al) overlies the primitive streak (ps) and was removed. (B) Epiblast (curved red arrow) continues to ingress into the primitive streak, so that, during whole embryo culture, operated conceptuses regenerate a new allantois (al-r) (C). (D,E) H/E-stained low- (D) and high- (E) magnification views of the posterior primitive streak immediately after removal of the allantois. The arrow in D indicates the anterior point of microcapillary entry into the yolk sac. Arrowheads in D and E indicate the site of removal of the allantois, just above the primitive streak. (F) H/E-stained 20-hour allantoic regenerate (al-r) contains mesothelium (m) and nascent endothelial channels (asterisks). (G-L) Immunostaining of allantoic regenerates and cultured unoperated controls. Histological sections immunostained with one antibody (G,H,J,K) were counterstained in hematoxylin. Doubly immunostained histological sections (I,L) were not counterstained. (G) FLK1 (brown color) in the endothelial plexus (e.g. asterisks) throughout the allantoic regenerate. (H) VCAM1 (brown color) in the mesothelium (m) of the distal allantoic two-thirds and a few distal core cells (arrowhead) of the regenerate. (I) FLK1 (blue color)/VCAM1 (brown color) double immunostaining reveals closely associated but separate populations of FLK1- and VCAM1-containing cells within the distal core, as previously reported (Downs et al., 2001). (J-L) Control unoperated host allantoises immunostained for (J) FLK1, (K) VCAM1 and (L) FLK1 (blue color)/VCAM1 (brown color). Other abbreviations: ac, amniotic cavity; am, amnion; ch, chorion; ec, ectoplacental cavity; x, exocoelomic cavity; ys, yolk sac. In F-L, embryo stages before and after culture are separated by '/'. Scale bars in L: 50 μm (E); 100 μm (F,G,I); 200 μm (D,H,J-L).

not specify allantoic mesoderm prior to its becoming the allantoic bud. Although outer cell morphology and expression of *Vcam1* alluded to the presence of mesothelium in the regenerates, flattening of distal outer cells cited as a provisional criterion for the onset of formation of mesothelium at the neural plate stage (Downs et al., 1998), was subjective and non-rigorous. Thus, electron microscopic analysis was used here to determine when and where junctional contacts, indicative of an epithelium, were present on the outer surface of the allantois.

The number of contacts between outer cells was scored in ultrathin sections of allantoises spanning the neural plate/early bud through 4-somite stages (Table 1). Three types of electron dense structures, including spot desmosomes, adhesive plaques and presumptive tight junctions (Batten and Haar, 1979), were identified at sites of contact at all stages (Fig. 3A-D), with neither the distal nor proximal halves favored (Table 1). Moreover, these structures were not always found in flattened cells. Finally, at the neural plate and headfold stages, the only junctional contacts observed in cells of the core were with outer cells (Fig. 3A), suggesting that the otherwise junction-free nascent core mesodermal cells shared ultrastructural similarities with migrating mesoderm rather than with epithelium (Batten and Haar, 1979).

Thus, the outer layer of allantoic mesoderm epithelializes as soon as the bud appears in the exocoelomic cavity. To obviate

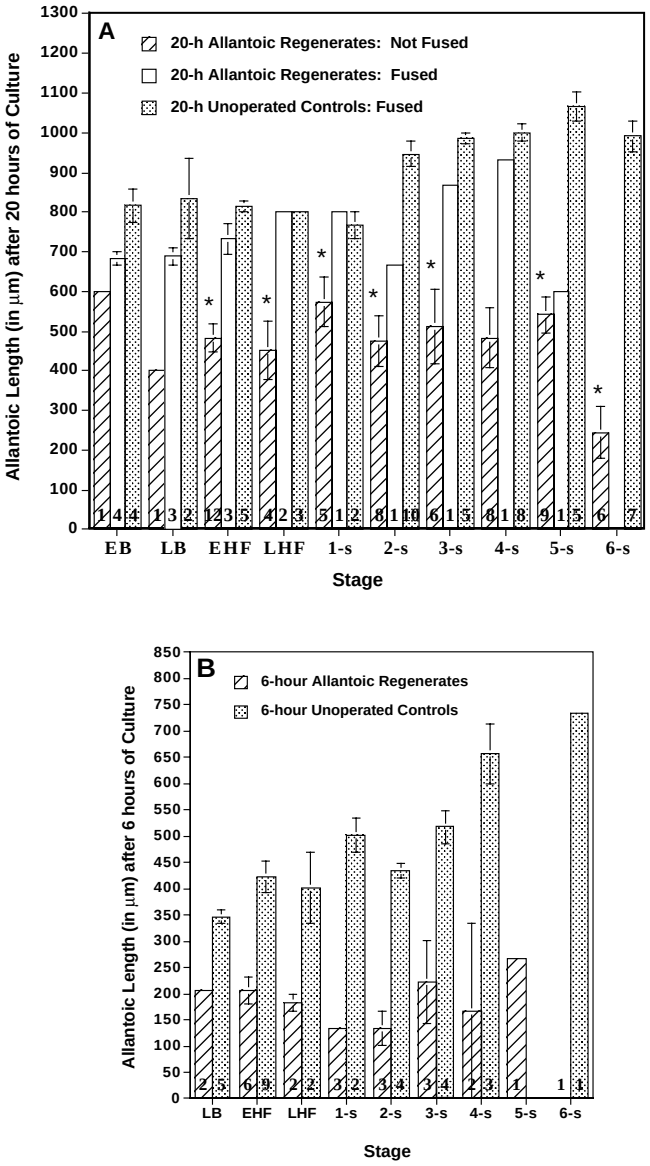

Fig. 2. Comparison of allantoic lengths in 20-and 6-hour regenerates and unoperated controls. Bar graphs of the length (in μm) of (A) unfused and fused allantoic regenerates, and control unoperated allantoises after 20 hours in culture, and (B) allantoic regenerates and control unoperated allantoises after 6 hours in culture, measured in the dissection microscope. Allantoic lengths were plotted against the developmental stage at which the culture period began. In B, the single regenerate created at 6-somite pairs was so small that it could not be accurately measured in the dissection microscope; thus, no bar is seen at this time point. The total number of allantoises scored in each category is indicated at the base of each column of the graph; vertical lines at the apex indicate the s.e.m.s; and asterisks in A indicate significant differences in length between unfused allantoic regenerates and unoperated control allantoises for each time point (P<0.05). Abbreviations: EB, neural plate/early allantoic bud stage; LB, neural plate/late allantoic bud stage; EHF, early headfold stage; LHF, late headfold stage; 1-6-s, 1- to 6-somite pairs.

dependence upon the electron microscope for detecting mesothelium in short-term regenerates (next section), immunohistochemistry was performed against cytokeratins,

Table 1. Evidence for allantoic mesothelium at the neural plate through 4-somite pair stages by transmission electron microscopy

Stage	Number of cell contacts	Number of cell contacts exhibiting junctional structures (%)	
		Proximal	Distal
EB	27	7 (25.9%)	7 (25.9%)
LB	52	13 (25%)	12 (23.1%)
EHF	114	18 (15.8%)	20 (17.5%)
LHF	79	15 (19%)	32 (40.5%)
4-s	105	41 (39%)	33 (31.4%)

One section per stage was scored.

Those sagittally-oriented sections exhibiting the longest length of the allantois, typically encompassing the midline of the allantois, were selected and subdivided into distal and proximal halves.

EB, neural plate/early allantoic bud; LB, neural plate/late allantoic bud; EHF, early headfold; LHF, late headfold; 4-s, 4-somite pairs.

found in many polarized cells. Cytokeratins were observed in the outer cells of the allantois as early as neural plate stages (Fig. 3E,F). However, by the headfold stage, cytokeratins were no longer confined to outer cells, but were also found in core allantoic cells (Fig. 3G), possibly in angioblasts undergoing endothelialization into nascent blood vessels.

Morphological and molecular differentiation in allantoic regenerates occurs with normal kinetics

To verify that differentiation took place with normal kinetics in allantoises post-microsurgical removal, 6-hour regenerates were created and analyzed for morphology and gene expression. As a prelude to this analysis, we first established the distance from the primitive streak at which VCAM1 appeared in ex vivo conceptuses (Fig. 4). VCAM1 was visible in distal mesothelial cells only when allantoises were at least 220.7 μm (±5.5 μm) long (data not shown; 1-somite pair; n=4). At 1-somite pair and all stages thereafter, the average length of the VCAM1-negative region was fixed at approximately 220.2 μm (±5.9 μm, n=34) (Fig. 4). This length did not differ significantly in conceptuses cultured for 20 hours (193.1±16.5 μm, n=9; P=0.08; data not shown), confirming that culture conditions did not alter correct topographical expression of *Vcam1*. The length of the VCAM1-negative region in fused regenerates was 192.4 μm (±12.8 μm; n=12; data not shown), similar to the unoperated cultured controls, whereas in unfused regenerates it was 149.5 μm (±8.0 μm; n=14; data not shown), significantly shorter than the controls (P=0.01). This difference may be attributable to the fact that once allantoises are anchored to the chorion, they may ‘stretch’ during subsequent enlargement of the exocoelomic cavity and lengthen; in the absence of anchoring to the chorion, ‘stretching’ would not occur in the unfused regenerates. Thus, after long-term culture, unfused regenerates might ultimately appear slightly collapsed and shorter.

In the next set of experiments, 6-hour regenerates were created (Fig. 2B, Fig. 5). Their average length before fixation was 177.6±19.2 μm (n=23; Fig. 2B). As we found that Bouin’s fluid and subsequent histological processing resulted in tissue shrinkage of 14.8% ±2.2% (n=14 fresh and subsequently fixed specimens, neural plate – 5-somite pair stages; data not shown), gene expression in the 6-hour regenerates was

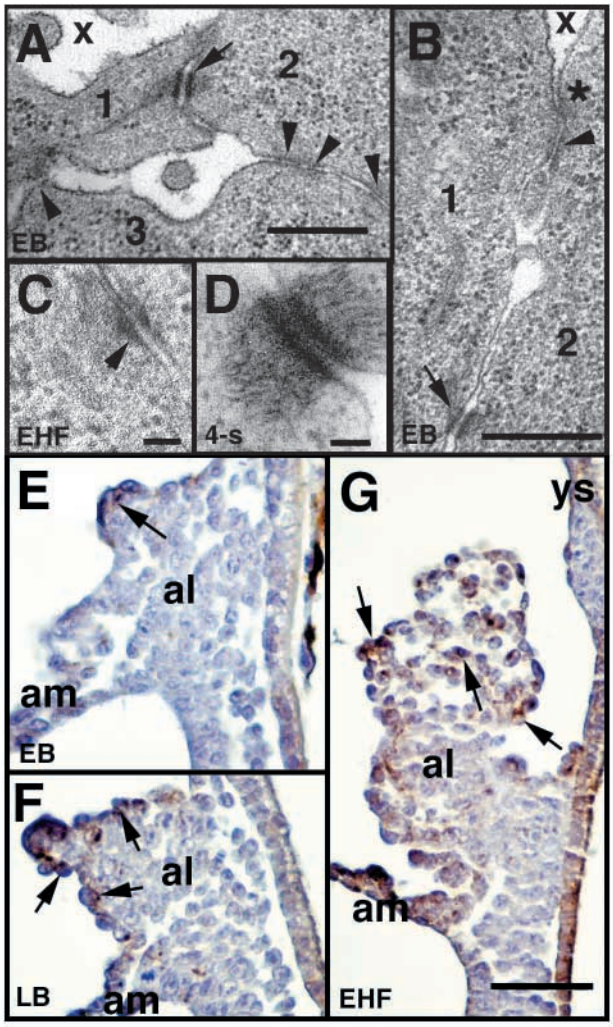

Fig. 3. Presence of mesothelium as detected by transmission electron microscopy and cytokeratins. (A-D) Transmission electron micrographs reveal various structural components of the plasma membrane at sites of cell-cell contact in outer cells of the allantois. (A) Ultrathin section through two outer cells (1,2), and an inner core cell (3) in the proximal region of an early allantoic bud (EB). The arrow points to a desmosome between the two outer cells, whereas the arrowheads indicate electron densities, possibly adhesion plaques or glancing sections through desmosomes, at sites of contact between the outer cells and an inner cell. Scale bar: 500 nm. (B) Ultrathin section contains a possible junctional complex between two cells (1,2) in the proximal region of an early allantoic bud (EB), consisting of a putative tight junction (left of asterisk), adhesion plaque (arrowhead), and spot desmosome (arrow). Scale bar: 500 nm. (C) Ultrathin section through the proximal region of an EHF stage allantois shows an isolated adhesion plaque very similar to those previously described (Batten and Haar, 1979). Scale bar: 100 nm. (D) Ultrathin section through the distal region of a 4-somite pair (4-s) allantois contains an apparently mature spot desmosome between two outer cells. Scale bar: 100 nm. (E-G) Brightfield photomicrographs exhibit immunostaining against cytokeratins (brown color, arrows) in nascent allantoises of ex vivo specimens. Sections were counterstained in hematoxylin. (E) EB stage. (F) LB stage. (G) EHF stage. Other abbreviations as in Fig. 1. Scale bar in G: 50 μm (E-G).

predicted to resemble that found in fixed ex vivo early headfold stages (Fig. 4).

Thus, after histological processing, several subsets of these 6-hour regenerates were then examined for gene expression and morphology. The average length of the first set of regenerates after fixation was 116.4 μm (±10.6 μm; 18 sections; *n*=6 specimens), with the longest one measuring 210.7±3.5 μm and the shortest one 88 μm. Although all of the unoperated controls contained distal VCAM1, in accord with their average length of 312.0±13.7 μm (Fig. 5C) (1-5-somite pairs, 13 sections; *n*=5 specimens, data not shown), none of the regenerates contained this protein (Fig. 5A,B). Thus, these results supported a minimal length requirement of 220 μm for *Vcam1* expression.

The presence of mesothelium was then confirmed in a second set of 6-hour regenerates by antibody staining against cytokeratins (Fig. 5D). As the average length of fixed 6-hour regenerates was similar to normal headfold-stage allantoises, described above, it was therefore not unexpected that cytokeratins were found in the regenerates' outer and inner cell populations, as reported in the previous section for expression of cytokeratins in ex vivo headfold-stage allantoises (Fig. 3G).

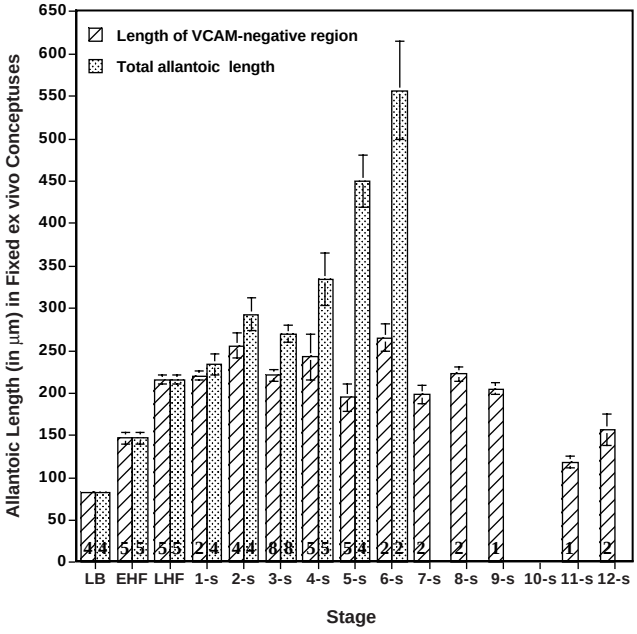

Fig. 4. The VCAM1-negative proximal region is approximately 220 μm long. The average total lengths (in μm) of allantoises and the VCAM1-negative proximal region from fixed ex vivo conceptuses were plotted as a function of developmental stage of the embryo. The number of allantoises examined at each time point is provided in the base of each bar; vertical lines at the top of each bar represent the s.e.m. Bars with only one specimen (9-s, 11-s) nonetheless contain errors, as measurements were the average of three histological sections for each allantois (see Materials and methods). After 6-somite pairs, the length of the VCAM1-negative region only is indicated because representation of the complete profile of fused allantoises was difficult to achieve in histological sections.

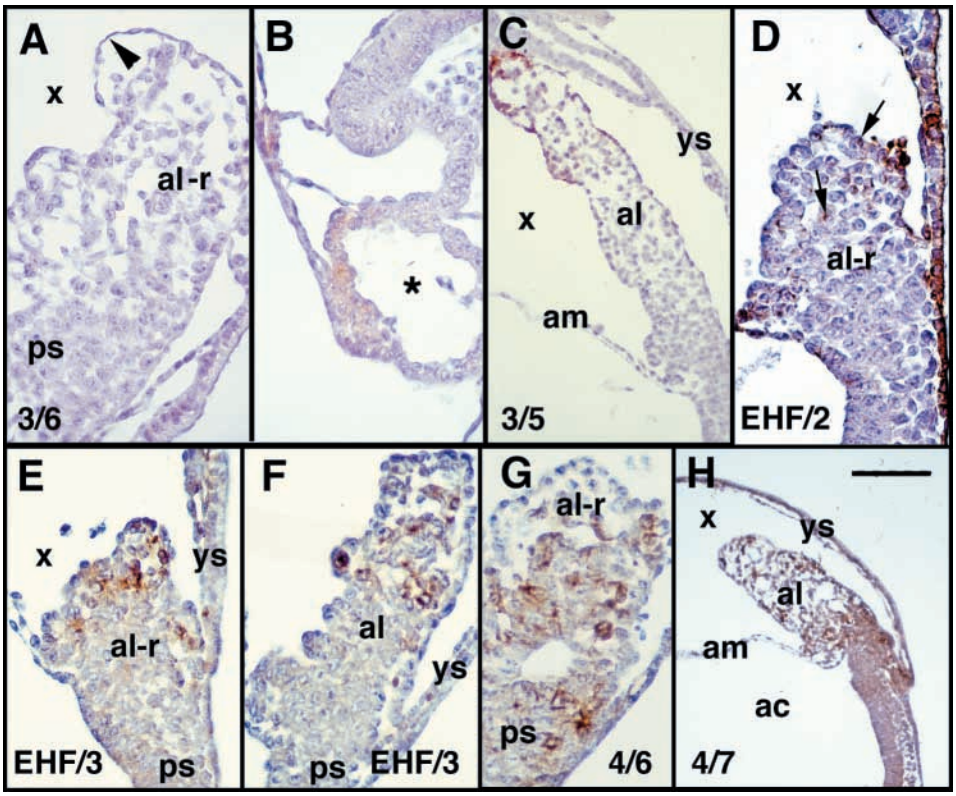

Fig. 5. Localization of VCAM1, cytokeratins and FLK1 in 6-hour allantoic regenerates. Allantoises were removed and operated conceptuses were cultured for 6 hours. Embryo stages before and after culture are indicated at the bottom of each panel (A,C-H), and are separated by '/'. Immunostain is brown in all panels; all sections were counterstained in hematoxylin. (A) Allantoic regenerate (al-r), 3/6-somite pairs, VCAM1-immunostained. This regenerate was less than 220 μm long and was negative for VCAM1 (i.e., no brown staining). Arrowhead indicates mesothelium. (B) Internal control, same conceptus as A, confirms the presence of VCAM1-positive cells in the heart (surrounding the asterisk) (Gurtner et al., 1995; Kwee et al., 1995). (C) VCAM1-stained unoperated cultured control allantois (al) from the same experiment as the specimen in A,B. (D) Brightfield photomicrograph shows cytokeratins (arrows) in both the allantoic mesothelium and core cells of the 6-hour regenerate (al-r). (E-H) Brightfield photomicrographs show FLK1 in the 6-hour regenerates (E,G) and corresponding unoperated cultured controls (F,H). Other abbreviations as in Fig. 1. Scale bar in H: 50 μm (A,B,D-G); 75 μm (H); 100 μm (C).

FLK1, which was previously observed in the distal core allantoic region between the late bud/neural plate and 2-somite pair stages (Downs et al., 1998), also showed distal staining in 6-hour regenerates created between the neural plate- and 2-somite pair stages; the primitive streak was also appropriately negative (Fig. 5E,F) (Downs et al., 1998). Not surprisingly, those regenerates created after 2-somite pairs did not exhibit regional polarity of FLK1 (Fig. 5G,H), as it was known that, by the time of microsurgery, the primitive streak region had become FLK1-positive, thereby making distal polarity of *Flk1* expression in these later regenerates impossible to discern (Downs et al., 1998).

Thus, taken together, our results revealed that allantoic regenerates behave like intact allantoises, no matter when they are formed: mesothelium was present, VCAM1 identified the chorio-adhesive cell type at a fixed and reproducible distance from the primitive streak, and endothelial cell formation began in the distal region during regeneration. On the basis of these observations, we conclude that specification of mesothelial, chorio-adhesive and endothelial cells does not occur within the primitive streak.

Differentiation within allantoic regenerates does not involve healing by yolk sac and amniotic mesoderm

Although the aforementioned observations provide compelling evidence that information intrinsic to the allantoic bud is responsible for re-establishing appropriate differentiation in the regenerates, an equally plausible mechanism could involve the adjacent yolk sac and/or amnion. Specifically, we hypothesized that, after removal of the allantois, the exposed primitive streak 'heals' by contribution of mesoderm from the yolk sac and amnion. The allantoic regenerate would then grow into and become coated in cells of yolk sac and/or amniotic origin (Fig. 6), which would then reorganize allantoic development. The molecular cue responsible could be the gene product of BMP4 as, in its absence, allantoises do not form or they are highly reduced in size and abnormal in morphology (Winnier et al., 1995; Lawson et al., 1999; Fujiwara et al., 2001). Moreover, both the yolk sac and amnion contain BMP4 (Lawson et al., 1999).

To investigate whether yolk sac and/or amniotic mesoderm and their associated BMP4 were involved in regeneration of allantoises, we first confirmed the presence of BMP4 in yolk sac and amniotic mesoderm at all time points (data not shown), in accord with previously defined BMP4 promoter-driven *lacZ* expression (Lawson et al., 1999). In the allantois, BMP4 was observed in many outer cells at neural plate stages (Fig. 7A, and data not shown), whereas the core was negative (data not shown). By the headfold stage, BMP4 was present in most cells throughout the distal allantoic third, as well as in much of the entire allantoic periphery to a depth of 1-3 cells (Fig. 7B, and data not shown from transverse sections of the allantois). This pattern remained relatively unchanged (Fig. 7B-E, and data not shown) until 6-somite pairs, at which time BMP4 was present throughout the allantois, and included both putative mesothelial and nascent endothelial cell populations (Fig. 7F, and data not shown), in agreement with an anecdotal in situ mRNA analysis of the allantois at approximately the same

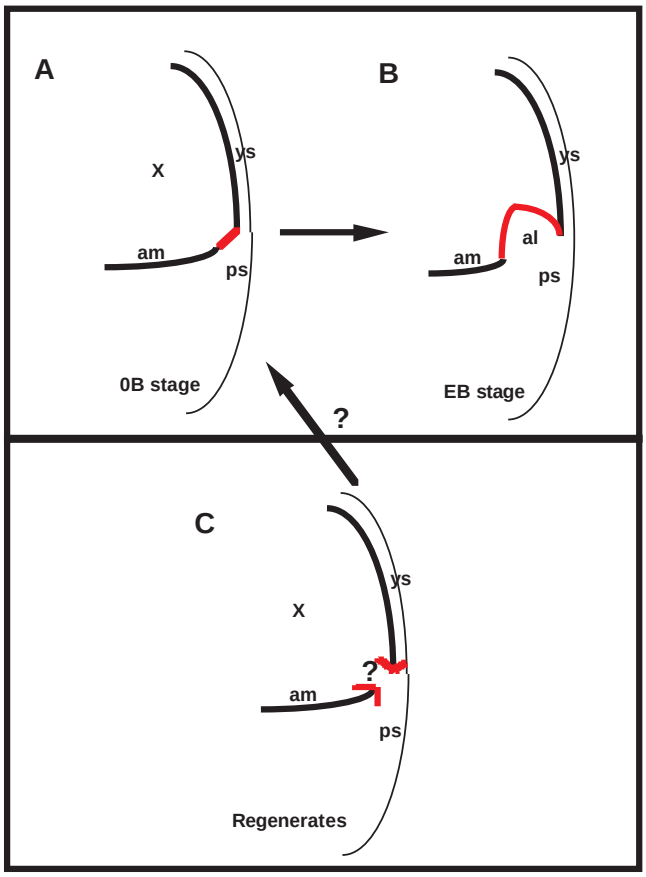

Fig. 6. Hypothetical model of growth of the allantoic bud and regenerates into BMP4-positive mesoderm of the exocoelomic cavity. Schematic diagram hypothesizes how growth of the allantois and allantoic regenerates might occur by a 'finger-in-a-glove' mechanism (suggested by Downs) (Downs, 1998). (A) Normal (non-hypothetical) neural plate/No bud (0B) stage, approximately 7.25 dpc. Thick lines (both black and red) are BMP4-positive with black color the mesodermal component of the yolk sac and amnion, and the red color the future site of the allantoic bud. The localization profile of BMP4 at this stage is from Lawson et al. (Lawson et al., 1999). (B) In this hypothetical scenario, the normal allantois grows into the BMP4-positive corner like a finger-in-a-glove, the result of which is an allantoic bud whose outer surface contains BMP4-positive cells. (C) The allantois has been microsurgically removed and, in the subsequent hypothetical scenario, BMP4-positive mesoderm from the yolk sac and amnion crawls onto the exposed primitive streak, thereby re-establishing the BMP4 expression pattern of the normal 0B stage in A, and subsequently that of B in the regenerates. Abbreviations as in Fig. 1.

stage (Mahlapuu et al., 2001). Between 7- and 16-somite pairs, these global patterns were little changed, and included robust levels of BMP4 at the chorio-allantoic fusion junction (Fig. 7G,H). Twenty-hour regenerates exhibited widespread BMP4 protein similar to that found in intact allantoises at ≥7-somite pairs (Fig. 7I).

To discover whether extrinsic BMP4, i.e. that from the yolk sac and/or amniotic mesoderm, was involved in restoring normal differentiation to the allantoic regenerates, we examined allantoises after regeneration from the headfold stage at 1-1.5-hour intervals between 0 and 6 hours (Fig. 7J-M).

Table 2. Proliferation of AlexaFluor594-conjugated Concanavalin A-labeled yolk sac mesodermal cells

Experiment	Well	Total number of labeled adherent cells (5 hours)	Total number of labeled adherent cells (20 hours)
1	1	623	1507
	2	568	1243
2	1	980	1746
3	1	366	1064
	2	310	491
Average		569.4	1210.2

See Materials and methods for details.

Although no evidence for BMP4 was found in the exposed primitive streak at time 0 hours (Fig. 7J), or in regenerating allantoises at 1.5 hours (Fig. 7K), BMP4 was clearly visible in peripheral and distal core cells of the regenerates at 3, 4 and 6 hours (Fig. 7L,M, and data not shown), thus resembling normal expression patterns. However, these results did not distinguish between BMP4 of extrinsic origin from BMP4 produced within the allantois itself.

To address this, the adjacent yolk sac and amniotic mesoderms were fate-mapped by labeling the mesodermal lining of the exocoelomic cavity with AlexaFluor-conjugated Concanavalin A, which selectively binds α-mannopyranosyl and α-glycopyranosyl residues of glyco-conjugates on the cell surface. First, to verify that ConA-labeled cells proliferated and passed their label on to progeny cells, single cell suspensions of the mesodermal and endodermal components of one of the tissues, the yolk sac, were plated onto tissue culture plastic (see Materials and methods). After 20 hours in culture, endodermal cells remained floating, and did not adhere to the plastic, in agreement with findings by others (R. Gardner, personal communication). In contrast, both labeled and unlabeled yolk sac mesodermal cells adhered to the plastic and had a vacuolated appearance (Fig. 8A-D). In three experiments, AlexaFluor ConA-labeled cells doubled in number over the 20-hour culture period (Table 2). We also confirmed that ConA-labeling did not inhibit mesothelial cell motility, by plating labeled allantoises (Downs et al., 2001) (Fig. 8E) and observing outgrowth at 8 (Fig. 8F) and 20 hours thereafter (data not shown). Moreover, the explants looked normal, in that they were well vascularized by 20 hours and morphologically similar to unlabeled controls, as previously described (Downs et al., 2001). Finally, use of ConA in these circumstances further revealed that allantoic outgrowth was mesothelial in origin.

After labeling exocoelomic mesoderm (Fig. 9A,B), allantoises were then removed and examined to verify that labeling was complete (Fig. 9C). Operated conceptuses were cultured for 8-12 or 20-24 hours alongside controls (Table 3). By 20 hours, most of the fluorescent label was localized to the distal region of intact labeled allantoises (Fig. 9D,E), in agreement with fate mapping studies which suggested that nascent allantoic mesoderm is displaced distally as fresh mesoderm is added by the streak (Lawson et al., 1991; Lawson and Pedersen, 1992; Downs and Harmann, 1997; Kinder et al., 1999). Although it might be argued that proximal cells died in the presence of ConA, we consider this unlikely, as the

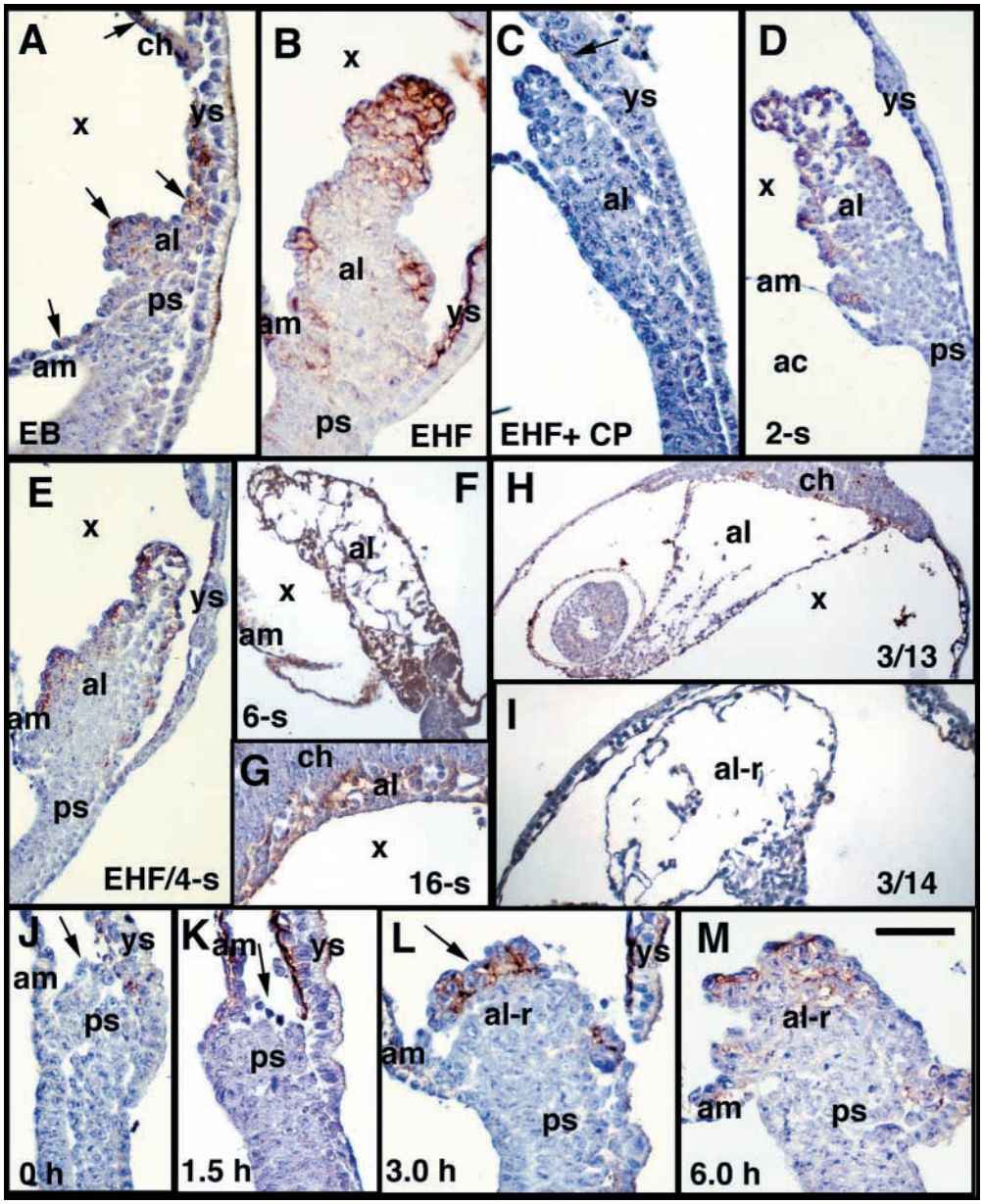

Fig. 7. Localization of BMP4 to the extraembryonic region of mouse gastrulae and allantoic regenerates. BMP4 (brown color) in the extraembryonic region of mouse conceptuses in ex vivo (A,B,D,F,G) and cultured unoperated (E,H) allantoises, and allantoic regenerates (I-M). Ex vivo control conceptus [pre-binding with control peptide, CP] (C). See text for complete explanation of staining patterns. In E,H,I, embryo stages before and after culture are separated by '/'. (A) EB stage. BMP4 is present in mesoderm lining the exocoelomic cavity and in the mesothelium surrounding the allantois at this stage, as shown in this glancing sagittal section through the lateral surface of an allantoic bud, in agreement with previous results (Lawson et al., 1999). In deeper sections, the core of the early bud was negative (data not shown). (B) EHF stage. (C) EHF stage, pre-binding antibody with control peptide (+ CP). The arrow indicates faint BMP4 in yolk sac mesothelium, suggesting that this amount of control peptide (100:1, CP:anti-BMP4) was not completely efficacious in pre-binding all antibody, although all other tissues were negative. (D) Two-somite pairs (2-s). (E) Cultured conceptus (EHF/4). (F) Six-somite pairs (6-s). BMP4 is now present throughout the allantois, including endothelium within the core. (G) Sixteen-somite pairs (16-s), BMP4 is present at the chorio-allantoic fusion junction. (H) Cultured conceptus (3/13); BMP4 is present in both mesothelium and in endothelial elements within the core. (I) Twenty-hour allantoic regenerate (3/14) demonstrates a similar BMP4 staining pattern in the allantois as that shown in H. (J-M) Time course of allantoic regenerates created from EHF-stage conceptuses shows BMP4 in the regenerates at (J) 0 hours, (K) 1.5 hours, (L) 3.0 hours and (M) 6.0 hours after allantoic removal. Arrows in J-L indicate the distal site of allantoic regeneration. Abbreviations as in Figs 1, 2. Scale bar in M: 50 μm (A-C,J-M); 100 μm (I); 150 μm (D-G); 200 μm (H).

allantoic explants of Fig. 8E,F were covered in labeled mesothelium at the end of the explant period.

In all six control conceptuses in which allantoises had been removed prior to labeling, label persisted in experimental regenerates, and was found laterally, rather than distally (Fig. 9F,G). Thus, we concluded that, if yolk sac and/or amniotic mesoderm crawled over the primitive streak, labeled cells might be expected in a lateral line, spanning the proximal to distal region of the regenerate. Of 72 experimental regenerates (Table 3), 23 were not scorable (see legend to Table 3). Of the remaining 49 regenerates, 28 were completely negative for AlexaFluor ConA (data not shown), whereas the other 21 regenerates contained just a few (2-10) positive cells (e.g. Fig. 9H,I) whose localization, though lateral, was not spatially consistent amongst the regenerates. Where regenerates were ≥266.8 μm long, all were well-vascularized and exhibited an outer layer of mesothelium (data not shown); where they were ≤200.1 μm long, all regenerates bore an outer layer of mesothelium, but they may or may not have contained an obvious vascular plexus (data not shown). The length of a small set of fresh 20-hour regenerates (403±47 μm; n=22) whose exocoelomic cavities had been ConA-labeled was compared with that of unlabeled regenerates (500±54 μm; n=6) from the same experiments (n=3), and found not to be significantly different (P=0.31). Moreover, four regenerates fused with the chorion (Table 3),

Table 3. AlexaFluor594-conjugated Concanavalin A in allantoic regenerates

Culture period	Number of regenerates examined	Number of regenerates not scored	Number of labeled regenerates	Number of negative regenerates
8-12 hours	8	3* (37.5%)	2/5 (40.0%)	3/5 (60.0%)
18-23 hours	64	20† (32.1%)	19/44 (43.1%)	25/44 (56.8%)
Total	72	23 (31.9%)	21/49 (42.9%)	28/49 (57.1%)

See Materials and methods for details.
*Two regenerates were fused to the yolk sac; 1 conceptus was dead.
†Twelve regenerates were too small to score (≤123.4 μm); 4 regenerates were fused with the chorion; 4 regenerates were fused to the yolk sac.

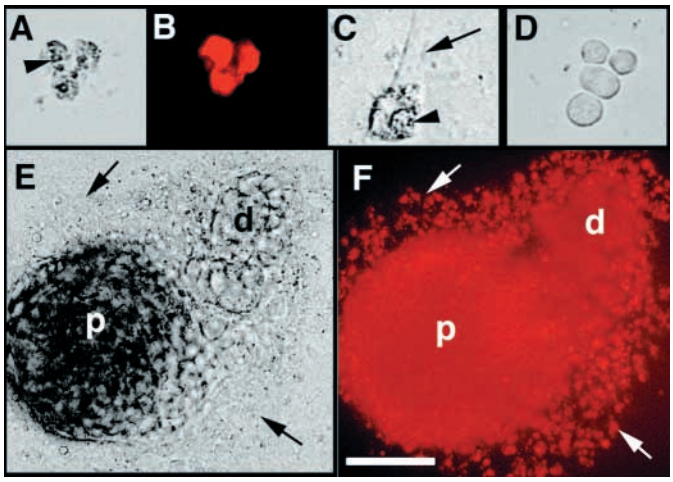

Fig. 8. AlexaFluor594-conjugated Concanavalin A does not affect mesodermal cell proliferation or mesothelial cell migration, and is inherited by daughter cells. Brightfield (A,C-E) and fluorescent (B,F) photomicrographs of AlexaFluor594-ConA-labeled yolk sac mesoderm and allantoic mesothelium. (A,B) ConA-labeled yolk sac mesodermal cells at 20 hours after culture. Arrowhead points to structures which give these cells a vacuolated appearance. (C) Control unlabeled yolk sac mesodermal cells, 20 hours after culture. Arrowhead points to 'vacuolated' region, whereas the arrow points to a filopodial projection often seen on both labeled and unlabeled cultured yolk sac mesodermal cells. (D) Example of a very minor cell population found in cultures of both labeled and unlabeled yolk sac mesodermal cells, but which were never labeled, and are thus possibly cells of blood island provenance. (E,F) ConA-labeled headfold-stage allantoic explant at 8 hours of culture. Arrows point to labeled mesothelial outgrowth. In this and Figs 9-11, d: distal, p: proximal. Scale bar in F: 50 μm (A-D); 100 μm (E,F).

confirming their functional competence despite the presence of ConA.

On the basis of these findings, we conclude that labeling the exocoelomic cavity of headfold- and early somite stage conceptuses with ConA has no detrimental affect on embryonic growth, embryonic differentiation or on allantoic regeneration. Although a very small number of yolk sac/amniotic cells may crawl over the exposed primitive streak and become incorporated into the lateral surface of the regenerates, failure to identify them in the majority of regenerates strongly suggests that differentiation in allantoic regenerates is not re-specified by a healing process that involves the adjacent yolk sac, amnion or BMP4 contained therein. Moreover, these results accord with previous ones, which investigated the fate of presumptive PGCs thought to reside in the base of the allantois (Ozdzenski, 1967); results of those studies demonstrated that cell movement at the posterior embryonic/extraembryonic junction is typically away from the streak, rather than toward it, the consequence of which is that re-entry of allantoic primordial germ cells into the fetus probably does not occur (Downs and Harmann, 1997; Anderson et al., 1999).

Proximal allantoic regions become VCAM1-positive following loss of contact with the streak

As described above, the 220 μm-long VCAM1-negative region remained fixed throughout allantoic development, suggesting either that the allantois acquires intrinsic information that limits the domain of VCAM1, or that the streak suppresses VCAM1 in the proximal allantoic region closest to it.

To investigate a role for the streak in suppressing VCAM1, whole donor allantoises were removed and placed into the exocoelomic cavity of hosts, either in normal or reversed orientation (Fig. 10), and cultured for 8 hours. We reasoned that, if the streak suppresses gene expression or translation of VCAM1 transcripts in cells closest to it, then the proximal region would exhibit VCAM1 upon release from contact with the streak.

Of 14 normally oriented grafts, 57% had fused with the chorion, 29% were lying flat across the chorion, 7% were free-floating in the exocoelom, and 7% had become wedged inside the yolk sac. Whatever the status of the allantoises, however, all 14 contained an uninterrupted layer of mesothelium and all displayed the VCAM1-negative proximal region, whereas the distal region was VCAM1-positive (Fig. 10A,C,D). Of the 28 reversed-polarity grafts, 50% exhibited proximal regions in contact with the chorion, 43% were lying across the chorion, and 7% were free-floating in the exocoelom. Despite their varied orientation, all looked identical to the intact controls, in that all contained mesothelium, and all proximal regions were negative for VCAM1 relative to the distal third (Fig. 10B). A separate set of experiments confirmed FLK1 throughout the length of the allantois, in accord with normal profiles in intact allantoises (Fig. 10H).

Allantoises were then removed and, based on measurements of the VCAM1-negative region (Fig. 4), cut into distal and proximal subregions. To ensure that the proximal regions fell to within at least one standard deviation of the average 220 μm VCAM1-negative region (data not shown), these were never longer than 150 μm. Proximal and distal allantoic subregions were then placed separately into the exocoelomic cavity of individual hosts, and cultured for either 8 or 24 hours.

All 8-hour proximal regions were negative for VCAM1 (Fig. 10E). Seven out of 24 proximal regions were free-floating in the exocoelom and 3/24 were tethered to the host's regenerated allantois (data not shown); all had formed a complete outer rind of mesothelium (Fig. 10E). Fourteen out of 24 proximal regions had undergone union with the chorion (data not shown), exhibiting mesothelium at the unfused edge and,

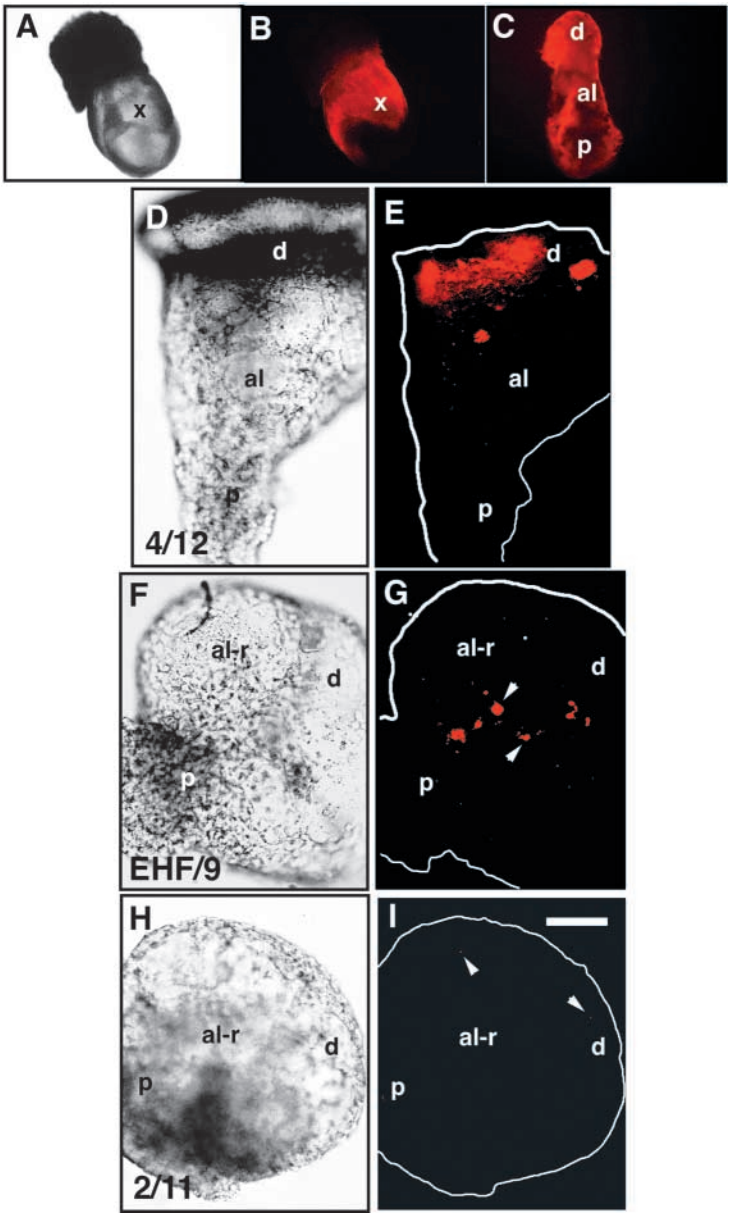

Fig. 9. Fate mapping the yolk sac and amniotic mesoderm with AlexaFluor594-conjugated Concanavalin A. Allantoises in D-I are from conceptuses that had been cultured for 20-24 hours and exposed on the same film to compare relative intensities of allantoic fluorescence within the same experiment. Embryo stages before and after culture in D-I are separated by a '/'. All panels contain gross microscopic views. (A-B) Posterior region of a LHF-stage conceptus in brightfield (A) and viewed by fluorescence after (B) labeling the exocoelomic cavity (x) with AlexaFluor ConA. (C) The allantois (al) has been removed from A to show complete superficial ConA labeling by fluorescence. (D,E) Cultured conceptus (4/12) in brightfield before (D) and in corresponding fluorescence (E). That most of the label is in the allantois and not the chorion was revealed by cutting the allantois away from the chorion and re-examining it (not shown). (F,G) Brightfield (F) and corresponding fluorescent (G) regenerated control allantois (EHF/9) in which the exocoelom had been labeled *after* removal of the allantois, thereby marking the posteriormost level of the streak. Arrowheads provide examples of very small individually labeled cells and patches of positive cells arranged in a lateral line spanning proximal to distal, typical of all six such 'pre-labeled' allantoic regenerates. (H,I) Brightfield (H) and corresponding fluorescent (I) images of an allantoic regenerate (2/11) (al-r) that contains two very small positive cells (arrowheads) in the distal region. Scale bar in I: 100 μm (C-I); 400 μm (A,B).

where they had made contact with the chorion, cells appeared to be breaking down (Downs, 2002). Of eight control distal regions, all were appropriately VCAM1-positive (Fig. 10F), with levels of VCAM1 approximating those of the intact controls (compare Fig. 10F with 10G). Both 8-hour distal and proximal regions were positive for FLK1 (Fig. 10I,J).

By 24 hours, 21/21 distal regions maintained VCAM1, with levels similar to intact allantoises (Fig. 11A). However, in contrast to the 8-hour explants, all 21/21 proximal regions had become VCAM1-positive throughout the mesothelium and core (Fig. 11B,C). One proximal region was tethered to the tip of the host's allantoic regenerate (Fig. 11B), and one had fused with both the chorion and the yolk sac (Fig. 11C). All the others had united with the chorion alone and behaved like distal subregions, with mesothelium breaking down at the fusion junction (data not shown). FLK1 localization was unchanged, being present in both the proximal and distal regions (data not shown). Further support for these observations was obtained by culturing subregions in suspension outside of the conceptus. Ten out of 10 distal and 10/10 proximal regions exhibited VCAM1 (Fig. 11D,E), whereas all 4/4 whole control allantoises were VCAM1-positive in both the outer mesothelial circumference and the core (Fig. 11F).

These findings suggest that a signal(s) emanating from the primitive streak or the allantoic mid-region suppresses proximal VCAM1 during normal allantoic development, but has no effect on formation of mesothelium or expression of *Flk1*. Once this putative factor(s) becomes inactive or depleted between 8 and 24 hours in the proximal isolates, VCAM1 is either induced or de-repressed.

To distinguish between signaling from the primitive streak and/or the allantoic midregion in inhibiting proximal VCAM1, distal allantoic thirds were excised from whole allantoises, maintaining continuity between the mid- and proximal regions ('mid/proximal'). In the same experiments, whole allantoises, distal and mid/proximal regions were cultured individually within the exocoelomic cavity of host conceptuses. As expected, distal thirds were always strongly VCAM1-positive (Fig. 11G). Moreover, not only was VCAM1 found throughout explanted whole allantoises (Fig. 11I), but it was also found throughout the mid/proximal subregions, although only two of these had remained free-floating in the exocoelom (Fig. 11H). Failure of the allantoic midregion to suppress proximal VCAM1 was confirmed in three additional experiments of isolated explants cultured in suspension for the same time period (data not shown).

On the basis of these observations, we conclude that the primitive streak limits the expression domain of VCAM1, confining the chorio-adhesive cell type to the distal allantoic

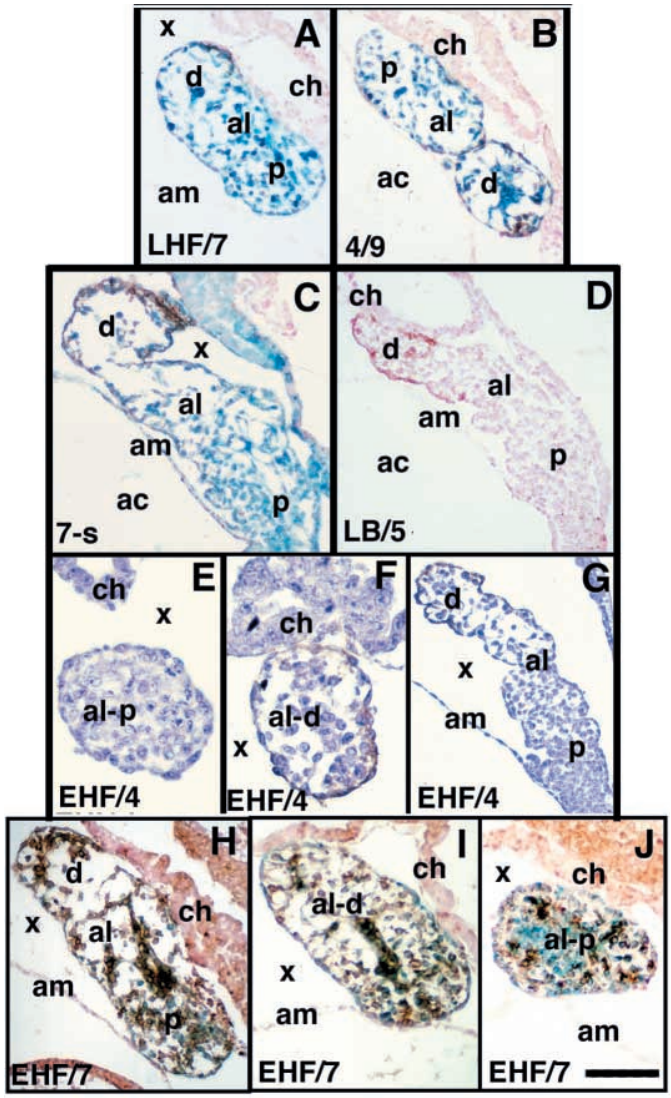

Fig. 10. VCAM1 and FLK1 in isolated whole allantoises and allantoic subregions after 8 hours of culture. Whole allantoises and allantoic subregions were placed into the exocoelomic cavity or in isolation in test tubes and cultured for 8 hours, after which they were VCAM1 (A-G) or FLK1 immunostained (H-J) (brown color). Allantoises from wild-type unoperated cultured (D,G) and/or *lacZ/+* ex vivo conceptuses (C) were used as controls. Sections were counterstained in nuclear fast red (A-D,H-J) or hematoxylin (E-G). In A-B, E-F and H-J, stages of synchronous donor allantoises and host conceptuses before and after culture are separated by a '/'. In D,G, stages of whole conceptuses before and after culture are separated by '/'. An ex vivo allantois is contained in C. (A) VCAM1 in distal region of whole X-gal-stained allantois in normal orientation. (B) VCAM1 is maintained in the distal region of a reversed polarity whole X-gal-stained allantois. The VCAM1-negative proximal region has made contact with the chorion. (C) Normal distal VCAM1 in X-gal-stained *lacZ/+* ex vivo control conceptus from the same experiment as A,B. (D) Wild-type unoperated cultured conceptus from same experiment as A-C shows normal distal VCAM1 in the allantois. (E-G) Allantoises are from wild-type conceptuses. (E) Proximal allantoic third does not contain VCAM1. (F) Distal two-thirds of the same allantois in E contains VCAM1. (G) Unoperated cultured control conceptus from same experiment as E,F. (H-J) Whole X-gal-stained allantois (H), X-gal-stained distal two-thirds (I), and X-gal-stained proximal third (J) of the same allantois in I exhibit FLK1 throughout the allantoic core. Abbreviations as in Figs 1, 2, 8. Scale bar in J: 50 μm (E,F); 75 μm (A,H-J); 100 μm (B-D,G).

region. In contrast, the streak is neutral with regard to formation of the mesothelium and endothelial-based vasculature.

Discussion

The goal of this study was to investigate the mechanism(s) by which the murine allantois differentiates into its major cell types. On the basis of findings reported here, we conclude that both the allantois itself and the primitive streak cooperate in normal allantoic development. Once the allantoic bud has formed, intrinsic factors appear to play a major role in specification of its endothelium, mesothelium and chorio-adhesive cells, whereas the posterior primitive streak may act to restrict the chorio-adhesive cells to the distal allantoic region by suppressing VCAM1 in proximal allantoic mesoderm.

The murine allantois acquires intrinsic information as the allantoic bud forms

That the allantois contains intrinsic factors responsible for its own differentiation was demonstrated by studying its regeneration. A combination of morphological and immunohistochemical approaches were used to demonstrate the normal kinetics of allantoic regeneration, including the invariable presence of mesothelium as defined by cytokeratins, a FLK1-positive endothelial plexus, and a defined VCAM1-positive distal region, indicative of the presence of chorio-adhesive cells. In addition, despite their smaller size, 20-hour regenerates were found to be competent to unite with the chorion. Repair of the exposed primitive streak from the adjacent yolk sac and amnion, possibly stimulated by BMP4 contained therein, was not consistently involved in allantoic outgrowth or in the re-establishment of proper morphological and molecular patterning in the regenerates. However, we cannot discount the possibility that BMP4, which was found in the normal allantoic bud and all of the regenerates (Fig. 7), may originate within the allantois and thereby contribute to its differentiation. Moreover, although cell age appears to play a major role in the timing of differentiation once the bud has formed, as discussed in the model below, the period during which proximal epiblast is converted into mesoderm within the streak plays no discernible role in specification of allantoic cell types.

These observations strongly suggest that, as the allantois becomes visible in the exocoelom, it acquires information that will direct its own differentiation.

The primitive streak establishes VCAM1's expression domain within the allantois

Although the streak does not specify the chorio-adhesive cells, it does appear to be involved in restricting their domain within the allantois by suppressing expression of *Vcam1* in the proximal allantoic region.

The base of the allantois, which corresponds with the

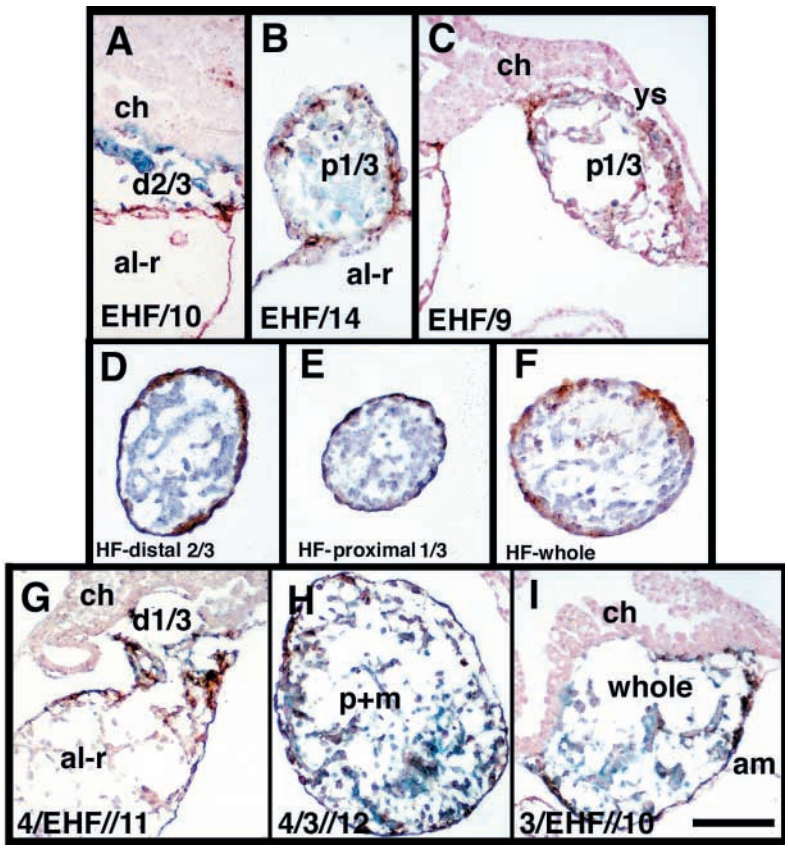

Fig. 11. VCAM1 immunostaining of isolated whole allantoises and allantoic subregions after 24 hours of culture. Subregions of whole *lacZ/+* donor allantoises were placed into the exocoelomic cavity of wild-type hosts (A-C,G-I), cultured for 24 hours, exposed to X-gal and VCAM1 immunostained (brown color). Wild-type allantoic subregions were cultured in isolation (D-F). Sections were counterstained with nuclear fast red (A-C,G-I), or hematoxylin (D-F). (A) Donor distal allantoic 2/3 has fused with the host's allantoic regenerate (al-r) and chorion exhibits VCAM1. (B) Donor proximal allantoic 1/3 is tethered to the host's allantoic regenerate (al-r) and exhibits robust VCAM1. (C) Donor proximal allantoic 1/3 is fused with both the host's yolk sac (ys) and chorion (ch) and exhibits robust VCAM1. (D-F) Wild-type distal 2/3 (D), wild-type proximal 1/3 (E), and whole wild-type allantois (F) from headfold (HF)-stage conceptuses were cultured in isolation for 24 hours; all exhibit robust VCAM1. (G) Donor distal allantoic 1/3 exhibits VCAM1 and is fused with the host's chorion. (H) Donor proximal/mid-allantoic region (p+m) is free-floating in the host's exocoelom and exhibited VCAM1 throughout the explant. (I) Donor whole allantois is fused with the host's chorion and exhibits strong VCAM1. In A-C, stages of synchronous donor allantoises and host conceptuses before and after culture are separated by a '/'. In G-I, initial stages of the asynchronous donor allantois and host conceptus are separated by '/', whereas the number after '//' indicates the final stage of the host after 24-hour culture. Scale bar in I: 50 μm (B); 75 μm (D-F); 100 μm (A,C,G-I).

posteriormost level of the streak, has previously been defined as the point of insertion of the allantois into the yolk sac and amniotic mesoderm (Ozdzenski, 1967) (reviewed by Downs, 1998). This definition has guided the present and all previous studies involving microsurgical removal of the allantois (Downs and Harmann, 1997; Downs et al., 1998; Downs and Bertler, 2000; Downs et al., 2001; Downs, 2002). Accordingly, measurements on histologically prepared allantoises revealed that VCAM1 was consistently localized to the distal region, beginning at a distance of 220 μm from the posterior limit of the primitive streak (Fig. 4). In isolation, proximal regions of allantoises were negative during the first 8 hours of culture, but by 24 hours they contained VCAM1 and behaved like distal tips in their ability to unite with the chorion (Fig. 11). Co-culture experiments revealed that suppression of *Vcam1* expression in the proximal region of the allantois was not because of its being in contact with its mid-region (Fig. 11).

On the basis of these data, we conclude that, although the primitive streak does not specify chorio-adhesive cells during formation of allantoic mesoderm, it does suppress VCAM1, either at the level of transcription or translation, in the proximal allantoic region once the bud has formed. Whether the mechanism of suppression involves direct cell contact and/or localized signaling from the streak remains to be determined.

Formation of allantoic mesothelium

On the basis of limited light microscopic data, we had previously supposed that formation of mesothelium began in the distal allantoic region (Downs et al., 1998). Thus, an unexpected finding in this study was the presence of this layer as soon as the bud appeared (Fig. 3). Moreover, mesothelium was found in all of the regenerates, as well as in explanted whole allantoises and allantoic subregions. These observations argue that mesothelium forms as a result of cues intrinsic to the allantois.

What those cues are is unknown, although it is tempting to speculate that they involve cells being on an outer surface. In other words, differentiation of mesothelium may share similarities with that of trophectoderm of the blastocyst, where differentiation of blastomeres along this lineage seems to depend upon being located externally (Tarkowski and Wroblewska, 1967). Thus, mesothelium of the allantois may differentiate by an inside-outside mechanism, as a result of formation of asymmetrical cell contacts between outer and inner cells. Indeed, in our limited study, outer and immediately subjacent inner cells were linked by junctional structures (Fig. 3A) that were not found anywhere else in the allantoic core during early stages. Intriguingly, the giant phosphoprotein, Ahnak, which is found near desmosomal contacts on epithelial cells (Hashimoto et al., 1995; Masunaga et al., 1995), was recently described on the allantoic surface (Kingsley et al., 2001). Ahnak was present there as early as the neural plate stage (Downs et al., 2002). Like uvomorulin which, along with one of its key modulators, protein kinase C (Winkel et al., 1990; O'Sullivan et al., 1993), has been implicated in blastomere polarization (Fleming et al., 1994), Ahnak is under the control of protein kinase B/C (Hashimoto et al., 1995; Sussman et al., 2001), and may thus localize to sites of cell-cell contact as outer cells epithelialize into mesothelium.

A model of allantoic differentiation

On the basis of these and previous findings, we propose a

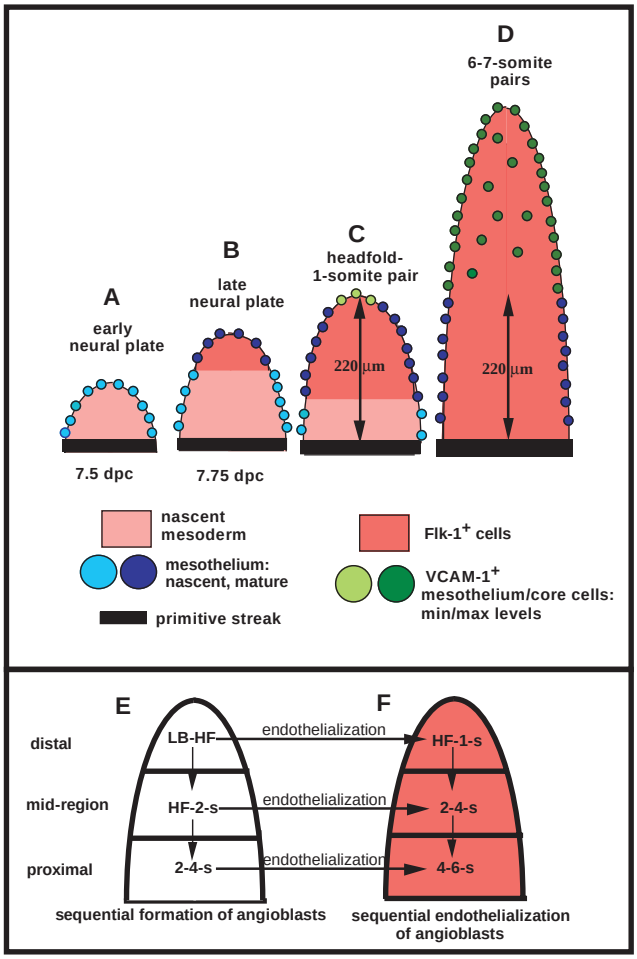

Fig. 12. Model of differentiation of allantoic mesoderm. (A) Mesoderm exits the primitive streak and is deposited into the exocoelom as the allantoic bud (light pink). We propose that allantoic mesoderm acquires intrinsic factors, possibly homeobox-encoded proteins, that initiate a series of downstream differentiative events. Outer allantoic cells exhibit junctional complexes, possibly based on their outside position, and form nascent mesothelium (light-blue circles). (B) Older core mesoderm (dark pink) and older mesothelial cells (dark blue) are displaced to the distal region as new mesoderm (light pink) emerges from the streak (Downs and Harmann, 1997). By this time, the series of downstream events initiated in A has progressed, as evidenced by *Flk1*-expressing angioblasts in the distal region (Downs et al., 1998) (dark pink). (C) FLK1 continues to spread proximally as older cells are displaced to distal regions because of the addition of new mesoderm through sustained streak activity (Downs and Bertler, 2000). At a distance of approximately 220 μm away from the streak, VCAM1 becomes visible in distalmost mesothelial cells (light-green color). Repression of VCAM1 in the proximal region may be the result of suppressive factors emanating from the streak. (D) Factors emanating from the streak continue to suppress VCAM1 to a distance of 220 μm whilst endothelium spreads proximally to the base of the allantois, at which time the allantoic vasculature amalgamates with those of the yolk sac and fetus (Downs et al., 1998) (not shown). Contribution of new mesoderm to the allantois from the primitive streak has slowed or ceased altogether (Downs and Bertler, 2000) (this study), levels of VCAM1 are at their most robust in the distal allantoic region (Downs, 2002) (dark green color), and chorio-allantoic union is nearing its maximal frequency (Downs and Gardner, 1995; Downs, 2002) (data not shown). After union with the chorion, the mesothelial surfaces of the allantois and chorion appear to break down, and the allantoic vasculature penetrates the chorionic ectoderm (Downs, 2002) (not shown). (E,F) Set of two schematic diagrams based on a previous study that described allantoic morphology (Downs et al., 1998) and spatiotemporal localization of FLK1 (Downs et al., 1998). The allantois is subdivided into distal, mid- and proximal regions. (E) Distal-to-proximal differentiation of allantoic mesoderm into angioblasts, the precursors of endothelial cells (Sabin, 1920) and which express *Flk1* (Yamaguchi et al., 1993). (F) Distal-to-proximal sequence of angioblast conversion into FLK1-positive endothelium. The horizontal arrows indicate the correlation between the time of formation of angioblasts for a given region in E with the time of formation of endothelium in F. It is thought that binding of Vascular Endothelial Growth Factor (VEGF) to its cognate receptor, FLK1, triggers epithelialization of allantoic angioblasts, resulting in formation of an endothelial cell plexus (Iwaguro et al., 2002). Although VEGF is secreted by mesothelium (Miquerol et al., 1999; Downs et al., 2001) and allantoic cells are responsive to VEGF (Downs et al., 2001), a spatiotemporal timecourse of VEGF and its isoforms has not been performed in the allantois. Abbreviations as in Fig. 2.

model of differentiation of allantoic mesoderm (Fig. 12). All of the data point to roles for intrinsic cues that may control allantoic cell age, as well as roles for cell position, and signaling from the posterior primitive streak.

Step 1: Emergence of the allantoic bud (Fig. 12A)

In the first step of allantoic development, nascent mesoderm exits the posterior primitive streak and is deposited into the exocoelom as the allantoic bud (Beddington, 1982; Beddington, 1983; Copp et al., 1986; Tam and Beddington, 1987; Kinder et al., 1999) (Fig. 12A, light pink). Outer allantoic cells acquire junctional complexes, possibly based on their exterior position, forming mesothelium (Fig. 3, Fig. 12A, light blue circles). In addition, allantoic mesoderm acquires intrinsic factors, possibly in the form of homeobox-encoded proteins, which may then trigger a cascade of downstream events controlling place- and time-dependent expression of morphoregulatory genes (Jones et al., 1992). Although systematic examination has been limited, expression of *Hox* genes encompasses several scenarios: it may begin in the allantois and spread to the streak (e.g. *Hoxb8/Hox2.4*) (Deschamps and Wijgerde, 1993; Deschamps et al., 1999; Forlani et al., 2003), it may begin in the streak and spread to the allantois (e.g. *Hoxa3/Hox1.5*) (Gaunt, 1988), or it may span both tissues (e.g. *Hoxc8/Hox3.1*) (Gaunt, 1988; Bieberich et al., 1990). Also, in some cases, *Hox* genes may be expressed only in the streak where they define an apparent border with the allantois (e.g. *Evx1*) (Dush and Martin, 1992; Crossley and Martin, 1995). Thus, the presence of a large number of *Hox* family members in both the allantois and primitive streak at critical times in differentiation of allantoic mesoderm make them prime suspects in regulation of the genetic and molecular regulatory pathways that control differentiation into the umbilical cord and chorio-allantoic placentation.

Step 2. The distal allantoic region differentiates into angioblasts (Fig. 12B)

Twelve hours after the bud appears, FLK1-positive angioblasts differentiate in the distal allantoic region, where mesoderm is oldest (Downs and Harmann, 1997; Kinder et al., 1999) (Fig.

12B, dark pink color). Several hours later, distal angioblasts coalesce into identifiable endothelial tubules (Downs et al., 1998) (Fig. 12E,F). The sequence of angioblast differentiation and endothelial tube formation then proceeds down the length of the allantois with striking regularity (Fig. 12E,F) (Downs et al., 1998), strongly suggesting that cell age plays a major role in this event. The importance of cell age is further underscored by uniform cell proliferation along the allantoic projection (Downs and Bertler, 2000); constant cell turnover could ensure that differentiation of each allantoic region takes place in turn. Moreover, whole explanted headfold-stage allantoises invariably vascularized with distal-to-proximal polarity according to a precise temporal program (Downs et al., 2001), and proximal allantoic subregions, which are initially relatively negative for FLK1 (Downs et al., 1998), also acquired abundant FLK1 in isolation (Fig. 10J) (this study).

Thus, a series of downstream genetic events would be activated until a final gene product triggers the expression of *Flk1* in the distal allantoic region, where mesoderm is oldest. Consequently, cell age, possibly the result of an internal timing mechanism initiated by *Hox* gene products in the bud (Fig. 12A), and cell position, ultimately coincide. An example of a candidate regulatory *Hox* gene is *Hoxb5*, whose product has been implicated in controlling expression of *Flk-1* (Wu et al., 2003), although its localization to the allantois has not yet been reported.

Step 3. Appearance of chorio-adhesive cells (Fig. 12C)

By 8.0 dpc, FLK1 is found in the distal two-thirds of the allantois (Downs et al., 1998) (Fig. 12E,F). Together with cell proliferation and cavitation, sustained activity of the streak results in lengthening of the allantois. Then, at a distance of approximately 220 μm from the streak, VCAM1 becomes visible in distalmost mesothelial cells (Fig. 12C, light green color). Thus, chorio-adhesive cells have formed.

Results of this and previous studies suggest a model of chorio-adhesive cell formation that, like endothelium, involves both cues intrinsic to the allantois and an internal timing mechanism (reviewed by Downs, 1998). In addition, signaling from the primitive streak appears to be involved (Figs 10, 11). Saitou et al. (Saitou et al., 2002) have suggested the presence of a localized signaling center within the posterior streak. Factors emanating from the posterior streak could be extended to the allantois, inhibiting expression of *Vcam1* in proximal mesoderm. A downstream target might be the homeobox-containing forkhead transcription factor, *Foxf1*, as in *Foxf1* mutants *Vcam1*'s expression domain is expanded to include the proximal allantoic region (Mahlapuu et al., 2001).

Step 4. The allantois contains a distal-to-proximal vascular network; distal regionalization of VCAM1 is maintained (Fig. 12D)

In this step, we propose that factors emanating from the streak continue to suppress VCAM1 to a distance of 220 μm. Endothelium has spread all the way down to the base of the allantois (Fig. 12D-F), at which time, the allantoic vasculature amalgamates with those of the yolk sac and fetus (Downs et al., 1998; not shown).

Chorio-adhesive cells

The VCAM1-negative proximal region may, in future, winnow out genes that regulate chorio-adhesive cell formation. For example, *Tbx4* nullizygous allantoises failed to grow far enough to fuse with the chorion and did not exhibit VCAM1 (Naiche and Papaioannou, 2003). In light of findings here, absence of VCAM1 may be due to the foreshortened mutant allantois' failure to escape the streak's suppressive influence, rather than to defective genetic interaction between *Tbx4* and *Vcam1*.

Intriguingly, despite a conspicuous absence of VCAM1, 8-hour proximal regions nonetheless often made contact with the chorion. Although the extent to which non-VCAM1- and VCAM1-containing proximal allantoic regions penetrate the chorion awaits further study, this observation is consistent with transgenic knockouts. These revealed that 50% of *Vcam1* nullizygous embryos undergo chorio-allantoic union before dying at approximately 11.5 dpc (Gurtner et al., 1995; Kwee et al., 1995). Potential explanations for this intriguing observation have already been discussed (Gurtner et al., 1995; Kwee et al., 1995; Downs, 2002).

Why VCAM1 is normally absent from the proximal allantoic region is not clear, but given that a major allantoic function is to unite with the chorion and form the umbilical vasculature, repression might ensure that the proximal region cannot fuse with the chorion. If it, like the distal region, spread along the chorionic surface (Downs, 2002), compression rather than elongation of the umbilical cord might occur. Although short cords are extremely rare, they are usually associated with fetal malformations (Benirschke, 1998).

Conclusions and future perspectives

Finally, although three cell types have thus far been characterized in the allantois, it is not known whether vascular smooth muscle cells arise from the allantois itself or are contributed to the allantois from the chorion. According to recent results (Yamashita et al., 2000; Motoike et al., 2003), vascular smooth muscle cells may originate from FLK1-positive precursor cells.

The function and origin of other cell types, known to exist only through gene expression patterns, remain unclear or unknown. For example, VCAM1-positive cells are closely associated with the FLK1-positive endothelium in the distal and not the proximal core, but their significance in allantoic development has not been elucidated (Downs et al., 2001; Downs, 2002). One possibility is that, once the chorio-allantoic fusion surfaces break down, VCAM1-positive distal cells bridge the connection between the FLK1-containing endothelial cells and the chorionic ectoderm (Downs, 2002), binding to α4-integrin present in the chorion (Bowan and Hunt, 1999). In addition to core VCAM1, α4-integrin has been identified in a small cell population in the proximal region of the allantois, which is continuous with the amnion (Downs, 2002). These cells may be involved, through integrin-mediated cell motility, in expanding the amnion during fetal growth.

The authors are grateful to Professor Richard Gardner for his suggestion of use of AlexaFluor-conjugated Concanavalin A for fate mapping yolk sac and amniotic mesoderm as well as for his most helpful comments on the final draft of the manuscript, to Professor Tom Fleming for a valuable discussion on trophectoderm formation, to Randy Massey and Ben August of the University of Wisconsin-Madison Medical School Department of Anatomy's EM Facility for expert preparation of conceptuses for electron microscopy, to Dr

Jacqueline Deschamps for help with *Hox* terminology, and to the anonymous reviewers for their very insightful and constructive criticisms. Grants HD036847 and HD042706 from the National Institutes of Health (K.M.D.) and a Hilldale Undergraduate Student Fellowship (E.H.) supported this study. Portions of this work will be submitted by Kimberly Inman in partial fulfillment of the Ph.D. requirements at the University of Wisconsin-Madison. Humane animal care was overseen by an institutional review board according to guidelines set by AALAC.

References

Anderson, R., Copeland, T. K., Scholer, H., Heasman, J. and Wylie, C. (1999). The onset of germ cell migration in the mouse embryo. *Mech. Dev.* **91**, 61-68.

Batten, B. E. and Haar, J. L. (1979). Fine structural differentiation of germ layers in the mouse at the time of mesoderm formation. *Anat. Rec.* **194**, 125-141.

Beddington, R. S. P. (1982). An autoradiographic analysis of tissue potency in different regions of the embryonic ectoderm during gastrulation in the mouse. *J. Embryol. Exp. Morph.* **69**, 265-285.

Beddington, R. S. P. (1983). The origin of the foetal tissues during gastrulation in the rodent. In *Development in Mammals*. Vol. 5 (ed. M. H. Johnson), pp. 1-32. Amsterdam: Elsevier Science Publishers.

Beddington, R. S. P. (1987). Isolation, culture and manipulation of post-implantation mouse embryos. In *Mammalian Development: A Practical Approach* (ed. M. Monk), pp. 43-70. Oxford: IRL Press.

Belaoussoff, M., Farrington, S. M. and Baron, M. H. (1998). Hematopoietic induction and respecification of A-P identity by visceral endoderm signaling in the mouse embryo. *Development* **125**, 5009-5018.

Bellairs, R. (1986). The primitive streak. *Anat. Embryol.* **174**, 1-14.

Benirschke, K. (1998). Remarkable placenta. *Clin. Anat.* **11**, 194-205.

Bieberich, C. J., Utset, M. F., Awgulewitsch, A. and Ruddle, F. H. (1990). Evidence for positive and negative regulation of the *Hox-3.1* gene. *Proc. Natl. Acad. Sci. USA* **87**, 8462-8466.

Bonnevie, K. (1950). New facts on mesoderm formation and proamnion derivatives in the normal mouse embryo. *J. Morph.* **86**, 495-546.

Bowan, J. A. and Hunt, J. S. (1999). Expression of cell adhesion molecules in murine placentas and a placental cell line. *Biol. Reprod.* **60**, 428-434.

Brown, J. J. and Papaioannou, V. E. (1993). Ontogeny of hyaluronan secretion during early mouse development. *Development* **117**, 483-492.

Chiquoine, A. D. (1954). The identification, origin, and migration of the primordial germ cells in the mouse embryo. *Anat. Rec.* **118**, 135-146.

Copp, A. J., Roberts, H. M. and Polani, P. E. (1986). Chimaerism of primordial germ cells in the early postimplantation mouse embryo following microsurgical grafting of posterior primitive streak cells in vitro. *J. Embryol. Exp. Morph.* **95**, 95-115.

Crossley, P. H. and Martin, G. M. (1995). The mouse Fgf8 gene encodes a family of polypeptides and is expressed in regions that direct outgrowth and patterning in the developing embryo. *Development* **121**, 439-451.

Deschamps, J. and Meijlink, F. (1992). Mammalian homeobox genes in normal development and neoplasia. *Crit. Rev. Oncog.* **3**, 117-173.

Deschamps, J. and Wijgerde, M. (1993). Two phases in the establishment of HOX expression domains. *Dev. Biol.* **156**, 473-480.

Deschamps, J., van den Akker, E., Forlani, S., de Graaff, W., Oosterveen, T., Roelen, B. and Roelfsema, J. (1999). Initiation, establishment and maintenance of *Hox* gene expression patterns in the mouse. *Int. J. Dev. Biol.* **43**, 635-650.

Downs, K. M. (1998). The murine allantois. *Curr. Top. Dev. Biol.* **39**, 1-33.

Downs, K. M. (2002). Early placentation in the mouse. *Placenta* **23**, 116-131.

Downs, K. M. and Bertler, C. (2000). Growth in the pre-fusion murine allantois. *Anat. Embryol.* **202**, 323-331.

Downs, K. M. and Davies, T. (1993). Staging of gastrulation in mouse embryos by morphological landmarks in the dissection microscope. *Development* **118**, 1255-1266.

Downs, K. M. and Gardner, R. L. (1995). An investigation into early placental ontogeny: allantoic attachment to the chorion is selective and developmentally regulated. *Development* **121**, 407-416.

Downs, K. M. and Harmann, C. (1997). Developmental potency of the murine allantois. *Development* **124**, 2769-2780.

Downs, K. M., Gifford, S., Blahnik, M. and Gardner, R. L. (1998). The murine allantois undergoes vasculogenesis that is not accompanied by erythropoiesis. *Development* **125**, 4507-4521.

Downs, K. M., Temkin, R., Gifford, S. and McHugh, J. (2001). Study of the murine allantois by allantoic explants. *Dev. Biol.* **233**, 347-364.

Downs, K. M., McHugh, J., Copp, A. J. and Shtivelman, E. (2002). Multiple developmental roles of Ahnak are suggested by localization to sites of placentation and neural plate fusion in the mouse conceptus. *Mech. Dev.* **119S**, S31-S38.

Dunwoodie, S. L. and Beddington, R. S. (2002). The expression of the imprinted gene Ipl is restricted to extraembryonic tissues and embryonic lateral mesoderm during early mouse development. *Int. J. Dev. Biol.* **46**, 459-466.

Dush, M. K. and Martin, G. M. (1992). Analysis of mouse Evx genes: Evx-1 displays graded expression in the primitive streak. *Dev. Biol.* **151**, 273-287.

Ellington, S. K. L. (1985). A morphological study of the development of the allantois of rat embryos in vivo. *J. Anat.* **142**, 1-11.

Fleming, T., Butler, L., Lei, X., Collins, J., Javed, Q., Sheth, B., Stoddart, N., Wild, A. E. and Hay, M. (1994). Molecular maturation of cell adhesion systems during mouse early development. *Histochemistry* **101**, 1-7.

Forlani, S., Lawson, K. A. and Deschamps, J. (2003). Acquisition of Hox codes during gastrulation and axial elongation in the mouse embryo. *Development* **130**, 3807-3819.

Friedrich, G. and Soriano, P. (1991). Promoter traps in embryonic stem cells: a genetic screen to identify and mutate developmental genes in mice. *Genes Dev.* **5**, 1513-1523.

Fujiwara, T., Dunn, N. R. and Hogan, B. L. (2001). Bone morphogenetic protein 4 in the extraembryonic mesoderm is required for allantois development and the localization and survival of primordial germ cells in the mouse. *Proc. Natl. Acad. Sci. USA* **98**, 13739-13744.

Gaunt, S. J. (1988). Mouse homeobox gene transcripts occupy different but overlapping domains in embryonic germ layers and organs: a comparison of *Hox-3.1* and *Hox-1.5*. *Development* **103**, 135-144.

Ginsburg, M., Snow, M. H. L. and McLaren, A. (1990). Primordial germ cells in the mouse embryo during gastrulation. *Development* **110**, 521-528.

Gurtner, G. C., Davis, V., Li, H., McCoy, M. J., Sharpe, A. and Cybulsky, M. I. (1995). Targeted disruption of the murine VCAM1 gene: essential role of VCAM-1 in chorioallantoic fusion and placentation. *Genes Dev.* **9**, 1-14.

Hashido, K., Morita, T., Matsushiro, A. and Nozaki, M. (1991). Gene expression of cytokeratin endo A and endo B during embryogenesis and in adult tissues of mouse. *Exp. Cell Res.* **192**, 203-212.

Hashimoto, T., Gamou, S., Shimizu, N., Kitajima, Y. and Nishikawa, T. (1995). Regulation of translocation of the desmoyokin/AHNAK protein to the plasma membrane in keratinocytes by protein kinase C. *Exp. Cell Res.* **217**, 258-266.

Iwaguro, H., Yamaguchi, J., Kalka, C., Murasawa, S., Masuda, H., Hayashi, S., Silver, M., Li, T., Isner, J. M. and Asahara, T. (2002). Endothelial progenitor cell vascular endothelial growth factor gene transfer for vascular regeneration. *Circulation* **105**, 732-738.

Jaquemar, D., Kupriyanov, S., Wankell, M., Avis, J., Benirschke, K., Baribault, H. and Oshima, R. G. (2003). Keratin 8 protection of placental barrier function. *J. Cell Biol.* **161**, 749-756.

Jolly, J. and Ferester-Tadié, M. (1936). Recherches sur l'œuf et de la souris. *Arch. D'Anat. Microsc.* **32**, 322-390.

Jones, F. S., Chalepakis, G., Gruss, P. and Edelman, G. M. (1992). Activation of the cytotactin promoter by the homeobox-containing gene Evx-1. *Proc. Natl. Acad. Sci. USA* **89**, 2091-2095.

Kaufman, M. H. (1992). *The Atlas of Mouse Development*. London: Academic Press.

Kinder, S. J., Tsang, T. E., Quinlan, G. A., Hadjantonakis, A.-K., Nagy, A. and Tam, P. P. L. (1999). The orderly allocation of mesodermal cells to the extraembryonic structures and the anteroposterior axis during gastrulation of the mouse embryo. *Development* **126**, 4691-4701.

Kingsley, P. D., McGrath, K. E., Maltby, K. M., Koniski, A. D., Ramchandran, R. and Palis, J. (2001). Subtractive hybridization reveals tissue-specific expression of ahnak during embryonic development. *Develop. Growth Differ.* **43**, 133-143.

Kwee, L., Baldwin, H. S., Shen, H. M., Steward, C. L., Buck, C., Buck, C. A. and Labow, M. A. (1995). Defective development of the embryonic and extraembryonic circulatory systems in vascular cell adhesion molecule (VCAM-1) deficient mice. *Development* **121**, 489-503.

Lawson, K. A. and Hage, W. (1994). Clonal analysis of the origin of primordial germ cells in the mouse. In *Germline Development*. Vol. 165 (ed. D. J. Chadwick and J. Marsh), pp. 68-84. Chichester: Wiley.

Lawson, K. A. and Pedersen, R. A. (1992). Early mesoderm formation in the

mouse embryo. In *Nato Advanced Study Workshop on Formation and Differentiation of Early Embryonic Mesoderm* (ed. R. Bellairs and J. W. Lash). New York: Plenum Press.

Lawson, K. A., Meneses, J. and Pedersen, R. A. (1991). Clonal analysis of epiblast fate during germ layer formation in the mouse embryo. *Development* **113**, 891-911.

Lawson, K. A., Dunn, N. R., Roelen, B. A., Zeinstra, L. M., Davis, A. M., Wright, C. V., Korving, J. P. and Hogan, B. L. (1999). Bmp4 is required for the generation of primordial germ cells in the mouse embryo. *Genes Dev.* **13**, 424-436.

Mahlapuu, M., Ormestad, M., Enerback, S. and Carlsson, P. (2001). The forkhead transcription factor Foxf1 is required for differentiation of extra-embryonic and lateral plate mesoderm. *Development* **128**, 155-166.

Masunaga, T., Shimizu, H., Ishiko, A., Fujiwara, T., Hasimoto, T. and Nishikawa, T. (1995). Desmoyokin/AHNAK protein localizes to the non-desmosomal keratinocyte cell surface of human epidermis. *J. Invest. Dermatol.* **104**, 941-945.

Miquerol, L., Gersenstein, M., Harpal, K., Rossant, J. and Nagy, A. (1999). Multiple developmental roles of VEGF suggested by a LacZ-tagged allele. *Dev. Biol.* **212**, 307-322.

Miura, Y. and Wilt, F. H. (1970). The formations of blood islands in dissociated-reaggregated chick embryo yolk sac cells. *Exp. Cell Res.* **59**, 217-226.

Motoike, T., Markham, D. W., Rossant, J. and Sato, T. N. (2003). Evidence for novel fate of Flk1+ progenitor: contribution to muscle lineage. *Genesis* **35**, 153-159.

Naiche, L. A. and Papaioannou, V. E. (2003). Loss of *Tbx4* blocks hindlimb development and affects vascularization and fusion of the allantois. *Development* **130**, 2681-2693.

O'Sullivan, D. M., Johnson, M. H. and McConnell, J. M. L. (1993). Staurosporine advances interblastomeric flattening of the mouse embryo. *Zygote* **1**, 103-112.

Ozdzenski, W. (1967). Observations on the origin of primordial germ cells in the mouse. *Zoologica Poloniae* **17**, 367-381.

Poelmann, R. E. (1981). The head process and the formation of the definitive endoderm in the mouse embryo. *Anat. Embryol.* **162**, 41-49.

Sabin, F. R. (1920). Studies on the origin of blood-vessels and of red blood-corpuscles as seen in the living blastoderm of chicks during the second day of incubation. *Contrib. Embryol.* **9**, 215-262.

Saitou, M., Barton, S. C. and Surani, M. A. (2002). A molecular program for the specification of germ cell fate in mice. *Nature* **418**, 293-300.

Schumacher, A., Faust, C. and Magnuson, T. (1996). Positional cloning of a global regulator of anterior-posterior patterning in mice. *Nature* **383**, 250-253.

Snell, G. B. and Stevens, L. C. (1966). Early embryology. In *Biology of the Laboratory Mouse* (ed. E. L. Green), pp. 205-245. New York: MacGraw Hill.

Sussman, J., Stokoe, D., Ossina, N. and Shtivelman, E. (2001). Protein kinase B phosphorylates AHNAK and regulates its subcellular localization. *J. Cell Biol.* **154**, 1019-1030.

Takahashi, Y., Imanaka, T. and Takono, T. (1996). Spatial and temporal pattern of smooth muscle cell differentiation during development of the vascular system in the mouse embryo. *Anat. Embryol.* **194**, 515-526.

Tam, P. P. L. and Beddington, R. S. P. (1987). The formation of mesodermal tissues in the mouse embryo during gastrulation and early organogenesis. *Development* **99**, 109-126.

Tarkowski, A. K. and Wroblewska, J. (1967). Development of blastomeres of mouse eggs isolated at the four- and eight-cell stage. *J. Embryol. Exp. Morph.* **18**, 155-180.

Wilt, F. H. (1965). Erythropoiesis in the chick embryo: the role of endoderm. *Science* **147**, 1588-1590.

Winkel, G. K., Ferguson, J. E., Takeichi, M. and Nuccitelli, R. (1990). Activation of protein kinase C triggers premature compaction in the four-cell stage mouse embryo. *Dev. Biol.* **138**, 1-15.

Winnier, G., Blessing, M., Labosky, P. A. and Hogan, B. L. M. (1995). Bone morphogenetic protein-4 is required for mesoderm formation and patterning in the mouse. *Genes Dev.* **9**, 2105-2116.

Wu, Y., Moser, M., Bautch, V. L. and Patterson, C. (2003). HoxB5 is an upstream transcriptional switch for differentiation of the vascular endothelium from precursor cells. *Mol. Cell. Biol.* **23**, 5680-5691.

Yamaguchi, T. P., Dumont, D. J., Conlon, R. A., Breitman, M. L. and Rossant, J. (1993). flk-1, an flt-related receptor tyrosine kinase, is an early marker for endothelial cell precursors. *Development* **118**, 488-498.

Yamashita, J., Itoh, H., Hirashima, M., Ogawa, M., Nishikawa, S., Yurugi, T., Naito, M., Nakao, K. and Nishikawa, S.-I. (2000). Flk-1-positive cells derived from embryonic stem cells serve as vascular progenitors. *Nature* **408**, 92-96.